ÇUKUROVA UNIVERSITY

INSTITUTE OF NATURAL AND APPLIED SCIENCES

MSc THESIS

Regional Analysis of Low Flow Using L-Moments for The Firat and Dicle Basins in Turkey Using L-Moments Approach and Plotting-Position Method

Mohammad MOSTO

Department of Civil Engineering

October, 2024

ÇUKUROVA UNIVERSITY

INSTITUTE OF NATURAL AND APPLIED SCIENCES

MSc THESIS

Regional Analysis of Low Flow Using L-Moments for The Firat and Dicle Basins in Turkey Using L-Moments Approach and Plotting-Position Method

Mohammad MOSTO

Department of Civil Engineering

This Master's Thesis was evaluated by the following Jury Members on 06/09/2024 and was approved by **unanimity/majority** of votes.

Jury : Prof. Dr. Recep YURTAL (Advisor) ……

: Prof. Dr. Neslihan SEÇKİN ……

: Assoc. Prof. Dr. Evren TURHAN ……

This thesis was written in the Department of Civil Engineering, Institute of Natural and Applied Sciences.
Thesis Number:

Prof.Dr. Sadık DİNÇER
Director Institute of Natural and Applied Sciences

Note: The usage of the presented specific declarations, tables, figures, and photographs either in this thesis or in any other reference without citation is subject to "The law of Arts and Intellectual Products" number of 5846 of Turkish Republic

CONTENTS

ABSTRACT I
ÖZ II
GENİŞLETİLMİŞ ÖZET III
ACKNOWLEDGEMENTS V
LIST OF TABLES VI
LIST OF FIGURES VII
ABBREVIATIONS VIII
1. INTRODUCTION 1
2. PREVIOUS STUDY 3
2.1. General Previous Studies 3
2.2. Applied Research in Turkey: 5
3. MATERIAL AND METHOD 9
3.1. Material 9
3.2. Method 11
3.2.1. Regional frequency analysis 11
3.2.2. Delineation of Homogeneous Regions 11
3.2.3. Discordance Measure 12
3.2.4. L-Moments Approach 12
3.2.5. A Comparison between Unbiased and Plotting-Position Estimators 14
3.2.6. Monte Carlo Simulation 15
3.2.7. Return Period, Probability, and Plotting Position 15
3.2.8. L-Moment Diagrams 16
.3.2.9. Identification of the regional distribution function 17
3.2.10. Z score calculation 18
3.2.11. Estimation of extreme quantiles associated with interest return periods 19
4. RESULTS AND DISCUSSIONS 21
4.1. Firat basin stations 21
4.2. The Dicle basin stations 30
5. CONCLUSION 39
REFERENCES 41
CURRICULUM VITAE 45

ÇUKUROVA UNIVERSITY

INSTITUTE OF NATURAL AND APPLIED SCIENCES

MSc THESIS

Regional Analysis of Low Flow Using L-Moments for The Firat and Dicle Basins in Turkey Using L-Moments Approach and Plotting-Position Method

Mohammad MOSTO

Advisor: Prof. Dr. Recep YURTAL

Department of Civil Engineering

ABSTRACT

Analyzing low flows is a new study in water resources engineering, especially with the occurrence of hydrological droughts over the last 20 years. The frequency analysis method is regularly used in estimating droughts and possibilities of low currents by finding a suitable distribution of recorded data about river flows.

This study aimed to determine regional frequency analysis for two catchment areas in Turkey; the first one was the Firat Basin, which contains about 20 rivers. The second one was the Dicle Basin, which has about 15 rivers. In both areas, two methods were applied for getting the L-moments to depend on the unbiased and plotting position methods. The heterogeneity measures, computed by carrying out 500 simulations using the data, showed that the two basins were identified as heterogeneous. Therefore, Firat basin was divided into three sub-regions and Dicle basin was divided into two sub-regions. It was also found that Gen. Logistic distribution was the most appropriate for most Firat and all Dicle basins.

Unbiased estimators demonstrated a slight advantage over plotting position estimators for quantile estimates in the Dicle and Firat basins, as reflected by RMSE values. Specifically, the average RMSE for the Firat region using unbiased estimators was 0.69, compared to 0.77 for plotting position estimators. The average RMSE for the Dicle region using unbiased estimators was 0.87, compared to 0.92 for plotting position estimators. This advantage of using Unbiased estimator was more evident in the upper quantile. However, due to being easier to compute the parameters depending on plotting position estimators, it may require further investigation to establish a critical threshold where they become preferable to unbiased estimators in larger sample studies.

Key Words: Regional frequency analysis, L-moments, Plotting position, Unbiased, Firat, Dicle

ÇUKUROVA ÜNİVERSİTESİ
FEN BİLİMLERİ ENSTİTÜSÜ

YÜKSEK LİSANS TEZİ

Türkiye'deki Fırat ve Dicle Havzalarında L-Momentlerle Düşük Akışın L-Moment Yaklaşımı ve Noktalama Pozisyon Yöntemiyle Bölgesel Analizi

Mohammad MOSTO

Danışman: Prof. Dr. Recep YURTAL

İnşaat Mühendisliği Anabilim Dalı

ÖZ

Hidrolojik kuraklık neticesinde ortaya çıkan düşük akışların analizi, son 20 yılda su kaynakları mühendisliğinde yeni bir çalışma haline gelmiştir. Frekans analizi yöntemi, kuraklık tahmininde sıklıkla kullanılan bir yöntemdir. Nehirlerde kaydedilen akış verilerine uygun olasılık dağılımları kullanılarak, meydana gelebilecek düşük akışların olasılıkları hakkında fikir elde etmek mümkündür.

Çalışmada, Fırat ve Dicle havzalarının Türkiye'de kalan kısmı için bölgesel frekans analizi gerçekleştirilmesi amaçlanmıştır. Fırat havzası yaklaşık 20 akarsu; Dicle havzası ise yaklaşık 15 akarsu içermektedir. Her iki bölgede de tarafsız tahmin edici ve noktalama pozisyon yöntemleri uygulanarak L-momentler elde edilmiştir. 500 tekrarlı Monte Carlo simülasyonu ile heterojenlik ölçüleri H(1), H(2) ve H(3) hesaplanmıştır. Ölçülere göre havzalar heterojen görülmektedir. Bu nedenle Fırat havza üç alt bölgeye ayrılmıştır ve Dicle Havza iki alt bölgeye ayrılmıştır. Ayrıca, Genelleştirilmiş Lojistik (GLO) dağılımının, Fırat havzalarının çoğu ve Dicle havzalarının tamamı için en uygun dağılım olduğu bulunmuştur.

Dicle ve Fırat havzalarındaki olasılıklar göz önüne alındığında, tarafsız tahmin tahmincilerinin, noktalama pozisyonu edicilere göre biraz daha avantajlı olduğu görülmektedir ve bu u durum, daha düşük RMSE değerleri ile belirginleşmiştir. Özellikle, Fırat bölgesi için tarafsız tahmin ediciler kullanılarak hesaplanan ortalama RMSE 0.69 iken, noktalama pozisyonu tahmin edicileri için bu değer 0.77 olmuştur. Dicle bölgesi için ise tarafsız tahmin ediciler ile ortalama RMSE 0.87 iken, noktalama pozisyonu tahmin edicileri için bu değer 0,92 olarak kaydedilmiştir. Tarafsız tahmin edicilerin bu avantajı, üst kantilde daha belirgin hale gelmiştir. Bununla birlikte, noktalama pozisyonu tahmin edicilerinin parametrelerinin daha kolay hesaplanması nedeniyle, daha büyük örneklem çalışmalarında tarafsız tahmin edicilere tercih edilecekleri kritik bir eşik için daha fazla araştırma yapılması gerekebilir.

Anahtar Kelimeler: Bölgesel frekans analizi**,** L-momentler, Noktalama Pozisyon, Tarafsız, Fırat, Dicle.

GENİŞLETİLMİŞ ÖZET

Hidrolojik kuraklıkla doğrudan alakalı olan düşük akışların analizi, özellikle son 20 yılda su kaynakları mühendisliğinde yeni bir çalışma haline gelmiştir. Çevresel açıdan düşük akışlar sonucunda, kirlilik yoğunluğu artmakta ve suda çözünmüş oksijen eksikliğinden dolayı balıkların ve diğer sucul canlılarının yaşamı tehlikeye girmektedir. Su yönetimi, düşük akışların tahmini, kentsel su, sulama suyu, hidroelektrik üretimi, su kalitesi kontrolü ve uzun süreli kuraklıkların ekosistemler üzerindeki etkilerinin incelenmesi açısından önemlidir.

Havzalardaki düşük akışları tahmin etmek için kullanılan iki farklı teknik vardır. İlk teknikte, akış verilerini belirlemek için havzanın fizyografik ve iklimsel özellikleri arasındaki ilişkiler kullanılır. İkinci teknikte, L-momentler yöntemiyle bölgesel frekans analizi yapılır. L-momentler yöntemi, daha doğru ve gerçekçi tahminler elde etmek için kullanılır ve parametre tahmini ile ilgili çeşitli sorunları çözebilir, heterojen bölgeleri ve en uygun dağılım fonksiyonunu tanımlayabilir.

Frekans analizi yöntemi, kuraklık tahmininde sıklıkla kullanılan bir yöntemdir. Bu yöntemle nehirlerde kaydedilen akış verilerine uygun olasılık dağılımı için birkaç defa meydana gelebilecek düşük akışların çeşitli olasılıkları hakkında fikir elde etmek mümkündür. Öngörülen bu düşük akışlar, yöneticileri kuraklığa karşı alınacak pratik önlemlere yönlendirebilir. Düşük akışları analiz etmek için ortalama yıllık akış, günlük ortalama akış, medyan akış ve en küçük mutlak akış gibi farklı endeksler kullanılır. Genel olarak, düşük akışların frekans analizi için belirli bir zaman aralığındaki (örneğin yedi gün) zaman serisi kullanılır. Bu endeks başta ABD ve İngiltere olmak üzere dünyanın birçok yerinde kullanılmaktadır. Bununla birlikte, L-momentleri yöntemi taşkın frekans analizine kıyasla düşük akış frekansında daha seyrek kullanılmaktadır.

Türkiye'deki 26 havzanın çoğunda veri eksikliği söz konusudur. Bu sebeple akış verilerini tahmin etmek için sentetik yöntemler sıklıkla kullanılmaktadır. Bununla birlikte, akış alanlarından toplanan verilerin uzunluğu arttıkça, akış değerlerini daha üstün olmayan olasılıklarla tahmin etmek için yeni yöntemler, istatistiksel analizlerle kombine edilmektedir. Yerinde ve bölgesel frekans analizlerinin yanı sıra L-momentler yöntemi kullanılarak çalışmalar yapılmaktadır. Bazı araştırmalarda yapay sinir ağları L-momentler yöntemiyle karşılaştırmış ve Türkiye'deki akış süreçleri için homojen bölgeleri tanımlamak için k-Ortalamalar kümeleme yöntemi kullanmıştır.

Bu çalışma ile Türkiye'deki 2 havza için bölgesel frekans analizinin gerçekleştirilmesi amaçlanmıştır. Birincisi yaklaşık 20 nehir içeren Fırat Nehri iken, ikincisi ise yaklaşık 15 nehir içeren Dicle Nehri'dir. Her iki bölgede de tarafsız tahmin edici ve noktalama pozisyon yöntemi uygulayarak, L-momentlerin nasıl elde edileceği konusunda iki yöntem kullanılmıştır. Veriler, Fırat Nehri boyunca yer alan 26 bölgede ve Dicle Nehri boyunca yer alan 14 bölgede minimum yıllık akış kayıtlarından oluşmaktadır. Bu veriler, Elektrik İsleri Etü İdaresi'nin 1957 ve 2007 arasında gözlediği akış kayıtlarından oluşmaktadır.

Her iki bölgede de tarafsız tahmin edici ve noktalama pozisyon yöntemleri uygulanarak L-momentler elde edilmiştir. 500 tekrarlı Monte Carlo simülasyonu ile heterojenlik ölçüleri H(1), H(2) ve H(3) hesaplanmıştır. Ölçülere göre havzalar heterojen görülmektedir. Bu nedenle Fırat havza üç alt bölgeye ayrılmıştır ve Dicle Havza iki alt bölgeye ayrılmıştır. Ayrıca, Genelleştirilmiş Lojistik (GLO) dağılımının, Fırat havzalarının çoğu ve Dicle havzalarının tamamı için en uygun dağılım olduğu bulunmuştur.

Uygun dağılım modelinin seçimi, doğru tahminler yapmak ve akış desenlerini anlamak için önemlidir. Bu nedenle, her bölge için frekans eğrileri ve bu eğriler için denklemler önerilmiştir. Tüm alt bölgeler için uygun dağılım kullanılarak T = 1.11, 1.25, 2, 5, 10, 25, 100, 200, 500 ve 1000 yıllık tekrarlama periyotları için standartlaştırılmış nicelikler hesaplanmış ve grafikle desteklenmiştir.

Dicle ve Fırat havzalarındaki olasılıklar göz önüne alındığında, tarafsız tahmin tahmincilerinin, noktalama pozisyonu edicilere göre biraz daha avantajlı olduğu görülmektedir ve bu u durum, daha düşük RMSE değerleri ile belirginleşmiştir. Özellikle, Fırat bölgesi için tarafsız tahmin ediciler kullanılarak hesaplanan ortalama RMSE 0.69 iken, noktalama pozisyonu tahmin edicileri için bu değer 0.77 olmuştur. Dicle bölgesi için ise tarafsız tahmin ediciler ile ortalama RMSE 0.87 iken, noktalama pozisyonu tahmin edicileri için bu değer 0,92 olarak kaydedilmiştir. Tarafsız tahmin edicilerin bu avantajı, üst kantilde daha belirgin hale gelmiştir. Bununla birlikte, noktalama pozisyonu tahmin edicilerinin parametrelerinin daha kolay hesaplanması nedeniyle, daha büyük örneklem çalışmalarında tarafsız tahmin edicilere tercih edilecekleri kritik bir eşik için daha fazla araştırma yapılması gerekebilir.

Her saha için tahminler, boyutsuz niceliklerin örneklem parametreleriyle çarpılmasıyla elde edilebilir. Ancak, bazı bölgelerde veri toplama sınırlıysa veya mevcut değilse, doğru frekans eğrilerini belirlemek zor olabilir. Bu duruma rağmen, bu bölgelerde minimum akış hızını ortalama akış sayesinde tahmin etmek mümkündür. Bu yöntem, herhangi bir tekrar dönemini aşmanın olasılığını dikkate alır. Her bölge için önerilen frekans eğrileri ve denklemlerin mevcut en iyi verilere dayandığını ve daha fazla veri mevcut olduğunda yenilenebilecek olduğunu unutmamak gerekir.

ACKNOWLEDGEMENTS

First and foremost, I would like to express my deep gratitude to God throughout my life.

I would also like to express my deep and sincere gratitude to my thesis supervisor, Prof. Dr. Recep YURTAL, for giving me the opportunity to do the thesis and providing invaluable guidance throughout this research. His vision, sincerity, and motivation have deeply inspired me. Besides my advisor, I would like to thank the rest of my thesis committee: Prof. Dr. Neslihan SEÇKİN and Assoc. Prof. Dr. Evren TURHAN, for their encouragement, insightful comments, and questions.

I am deeply grateful to my parents for their love, prayers, care, and the sacrifices they made to provide me with an education. I extend heartfelt thanks to my wife, Hasnaa, and my sons, Samir and Rayan, for their love, understanding, prayers, and continuous support throughout the completion of this thesis. I also wish to express my sincere appreciation to my research colleague, Mohammad WES, for his consistent support.

Lastly, I would like to extend my gratitude to all those who have supported me, both directly and indirectly, in completing this thesis.

LIST OF TABLES

Table 3.1. Basins in Turkey and their characters 10
Table 3.2. Type of distribution 17
Table 4.1. Used Stations in Firat Basin 21
Table 4.2. L-Moments values for the Firat basin depending on plotting position estimators. 24
Table 4.3. L-Moment Values for the Firat basin depending on unbiased estimators. 25
Table 4.4. Results of heterogeneous test for Firat basin. 25
Table 4.5. Z Test's Results for Firat basin 26
Table 4.6. Quantile Function for Firat Basin depending on Plotting Position estimators. 26
Table 4.7. Quantile Function for Firat Basin depending on Unbiased estimators. 27
Table 4.8. Accuracy Measures of the Regional Growth Curve for the Firat Region depending on Plotting Position estimators. 28
Table 4.9. Accuracy Measures of the Regional Growth Curve for the Firat Region depending on Unbiased estimators. 28
Table 4.10. Used Stations in Dicle Basin 30
Table 4.11. L-Moments Values for the Dicle Basin depend on plotting position estimators. 32
Table 4.12. L-Moment Values for Dicle basin depending on unbiased estimators. 33
Table 4.13. Result of heterogeneous test for Dicle basin. 33
Table 4.14. Z Test's Results for Dicle basin. 34
Table 4.15. Quantile Function for Dicle Basin depending on Plotting Position estimators. 34
Table 4.16. Quantile Function for Dicle Basin depending on Unbiased estimators. 35
Table 4.17. Accuracy Measures of the Regional Growth Curve for the Dicle Region depending on Plotting Position estimators. 35
Table 4.18. Accuracy Measures of the Regional Growth Curve for the Dicle Region depending on Unbiased estimators. 36
Table 5.1. RMSE values in each of the subregions for the Upper Quantile and the Lower Quantile. 39

LIST OF FIGURES

Figure 3.1. Basins in Turkey (CografyaHarita, 2017).....10
Figure 3.2. C_{kl}- C_{sl} diagram and the curves of distributions.....18
Figure 4.1. Geographical distribution of stations in the Firat basin. 22
Figure 4.2. The relationship between $\boldsymbol{\tau_1}$ and $\boldsymbol{\tau_3}$ for all station in Firat Basin 23
Figure 4.3. The relationship between $\boldsymbol{\tau_1}$ and $\boldsymbol{\tau_3}$ for sub regions in Firat Basin. 23
Figure 4.4. Frequency Curves of the Firat Basin depend on Plotting Position and Unbiased estimators. 29
Figure 4.5. Geographical distribution of stations in the Dicle basin.....31
Figure 4.6. The relationship between $\boldsymbol{\tau_1}$ and $\boldsymbol{\tau_3}$ for all stations in Dicle Basin 31
Figure 4.7. The relationship between $\boldsymbol{\tau_1}$ and $\boldsymbol{\tau_3}$ for subregions in Dicle Basin. 32
Figure 4.8. Frequency Curves of Dicle Basin depend on Unbiased estimators and Unbiased estimators. 37

ABBREVIATIONS

μ : Mean of a frequency distribution

a_r, B_r : rth probability weighted moment of a frequency distribution

Cv : Coefficient of variation of a frequency distribution

Di : Discordancy measure for a site i in a region

H : Heterogeneity measure for regional data

K : Kurtosis of data sample.

l_r : rth L-moment of a data sample.

S : Standard deviation of a data sample.

t : L-cv of a data sample.

t_r : rth L-moment ratio of a data sample.

Var ( ) : Variance of a random variable.

Z : Goodness of fit measure for regional data.

1. INTRODUCTION

Having the occurrence of hydrological droughts in the last 20 years, analyzing low flows has become a new study in water resources engineering. As a result of low flows in the environment, pollution density increases, and the life of fishes and other aquatic creatures is endangered due to the lack of dissolved oxygen in the water. In terms of water management, estimating low flows is important for urban water, irrigation water, hydroelectric production, water quality control, and examining the effects of long-term droughts on ecosystems (Modarres 2008). The frequency analysis method is regularly used in estimating droughts; it is possible to give an idea about various possibilities and low currents that may occur in recurrence times for a distribution suitable for the flow data recorded in rivers. The prediction of low flows might lead managers to take practical arrangements against drought. Different indices, such as the average annual flow, the daily average flow, the median flow, and the least absolute flow, are used to analyze low flows. Generally, the temporal series of low annual flows are used in a certain time interval (e.g., seven days) for the frequency analysis of low flows (Kil & Sang 2008). This index has been used widely, especially in the USA and UK (Smakhtin 2001).

The origin of the science of statistics of extreme values dates back to the 19th century. There are many references in which the problem of finding a distribution model of maximum and minimum values in a statistical population arises. As one of the greatest achievements in the first half of the 20th century, the demonstration that there are only three parametric families of limit probability distributions is mathematically compatible with the study of extreme values (Fisher and Tippett, 1928).

Afterward, more studies have been done by different authors in putting the foundations of the study of the distribution of extreme values. The main result of this work was concluded by the publication of the book Statistics of Extremes (Gumbel, 1958) which is one of the most important milestones in the history of the theory of extreme values. Since then, this theory has contributed to the advancement of many science and engineering fields, such as hydrology of extreme values and its application of predicting the frequency of river flooding.

Although the information used in this research has been taken from a certain gauging station over many years, many hydrologists have shown concerns about the associated drawbacks with the local methodology. The short duration of the available maximum flow observations series and the rare occurrence of extreme flows cause the flow estimation provided by the local analysis to have high uncertainty. That is why, for decades, different procedures have been emerging focused on trying to solve the limitations associated with the short temporal length of the records by applying different regional approaches to alleviate the lack of data in time with the abundance in space.

The index flood procedure (Dalrymple, 1960) supports the regional methodology by assuming that the same frequency distribution is applied for the basins belonging to a certain region

previously considered homogeneous except for a scale factor. A decade later, the development of regional frequency analysis got great advance through the formulation proposed by Hosking and Wallis, with a methodology based on the index flood procedure and the incorporation of the parameter estimation approach of distribution functions through L-moments (Hosking and Wallis, 1997).

Low-flow statistics are critical for successful water resource planning and management in ungauged or poorly gauged catchment areas. The primary objective of frequency analysis is to use probability distributions to link the magnitude of extreme events with their corresponding frequency distributions.

Low flow frequency was investigated using annual minimum daily streamflow data for Turkey's Firat and Dicle basins. This research aimed to find the probability distribution which best fits the streamflow data and calculates the return duration of extremely low-flow episodes. The L-moment approach was used to determine the probability parameter using distributions such as Gamma, LN3, GEV, PE3, GLO, and Kappa.

Data from two catchment areas in Turkey were used. The first one was the Firat Basin, which contains about 20 rivers. The second one was the Dicle Basin, which has about 15 rivers. In both areas, two methods were applied to get the L-moment values: unbiased and plotting position methods.

2. PREVIOUS STUDY

2.1 General Previous Studies

In the last 20 years, analyzing low flows with the occurrence of hydrological droughts has become a new study of water resources engineering. In terms of the environmental consequences, as pollution density increases because of low flows and a lack of dissolved oxygen in the water, fish and other aquatic creatures' lives are threatened. In terms of water management, estimating low flows is important in analyzing urban water, irrigation water, hydropower generation, water quality control, and the effects of long-term droughts on the ecosystem.

The first group of techniques was used to estimate low flows in basins without flow data. In this technique, the relations between the physiographic and climatic features of the basins, which are the hydrological properties, are used to determine the flow (both flood and low flow) data of the basin without data from the relations. In this technique, the homogeneity of the basins depends on one or more of their features (geology, climate, physiography, and hydrology). Homogeneity research in basins is carried out by group analysis. In classical grouping methods, basins with different characteristics can be grouped according to the degree of unit membership. However, if the characteristics of the stations are similar, the basin can be analyzed without splitting into sub-basins or other groups.

On the other hand, the fuzzy group analysis method allows a station to have few memberships or to be distributed across all groups. Due to this advantage, fuzzy group analysis has been used in regionalization studies in recent years. In a study conducted in Kingdom Province by Hall et al. (1999), 101 stations in two regions were examined with fuzzy systems and the BCO (fuzzy C-Means) method. In (Jingyi & Hall 2004), eighty-six stations were examined using flood frequency analysis by the BCO method in China. In this study, homogeneous regions were found with the help of statistics suggested by Hosking & Wallis (1997).

Regional frequency analysis is the second technique for studying this type of problem. More accurate and realistic forecasts are obtained by collecting station information with long-term data using the L-moments method. The L-moments method solves various problems related to parameter estimation, zoning, and distribution definition. L-moments are linear combinations of probability-weighted moments (PWM). However, it is easier to explain the distribution's shape measurement with the L-moments method than with the probability-weighted moment method. This method can summarize the statistical distribution more meaningfully and show smaller variations. (Hosking & Wallis, 1993) and many other researchers have developed numerous tests using L-moment diagrams to define regional distributions.

The L-moments method has been applied less frequently in low-flow frequency analysis compared to flood flow frequency analysis (Eslamian and Chavoshi, 2003; Malekinezhad et al., 2011). Pearson (1995) applied the L-moment charts for about 500 watersheds in more than 1455

river areas to find suitable potential distributions for modeling New Zealand's annual minimum flow chain. A definition based on "meteorology" in 28 countries showed that the LN3 distribution is not standard in any country, GEV is standard in one country, and LP3 is a standard in seven countries.

Since its start, numerous studies have been interested in low-flow frequency analysis using the L-moments method (Hosking, 1990). The aim was always to estimate the goodness-of-fit of different probability distributions to regional data. For example, Kroll & Vogel (2002) used the L-moment ratio chart to determine the probability distribution of a low flow in the USA. Pearson III (PIII) and LN3 are recommended as distributions to accommodate low flows in intermittent and uninterrupted locations. Minocha (2002) argued that the choice of probability distribution should depend not only on the graph of L-moment diagrams but also on the appropriate fitness scale presented by Hosking & Wallis (1997), which is directly related to L moments. The Minocha method includes computing summary statistics from the data and then testing whether their values are compatible with random simulation chains based on a chosen distribution.

Caruso (2000) used L-Moment to assess the suitability of 21 rivers in the Otago region of southern New Zealand and to select the best minimum flow allocations. They found that the GEV distribution was the best for a potential site group in Otago. Kroll and Vogel (2002) applied the L-moment method to recognize the likelihood of a low-flow chain in the USA. It was suggested that Pearson III (PIII) and LN3 are suitable probability distributions. Minocha (2003) indicated that the appropriate probability distribution is selected using the L-moments diagram and the goodness-of-fit measurement, as Hosking and Wallis (1997) described.

Bayazit and Onoz's (2002) used L-Moment to forecast different probability distribution parameters fitted with a 36-year record of the 7-day annual minimum flow in the Trent River basin in the UK. Then they compared the results obtained with those produced by the L-moment method. Chen et al. (2006) showed that the results of the regional frequency analysis of low-flow using the L-ratio graph might satisfy practicality. The natural logarithmic distribution of three parameters was the best probability distribution for the Dongjiang River in Hong Kong.

Peng et al. (2009) demonstrated that the use of L-moments for low-flow analysis in the karst region of southwest China yielded reliable results, with the Generalized Logistic (GLO) distribution being the most suitable. Similarly, Shi et al. (2010) applied L-moments for regional frequency analysis to assess low flow in the same karst region. Their findings, based on the L-moments ratio diagram, Zdist, and t4 statistic criteria, confirmed the robustness of the GLO distribution for the area. Dodongeh et al. (2013) also employed L-moments for low-flow frequency analysis at ungauged sites in the Sefidroud basin, located in northwestern Iran.

Keshtkar (2015, p. 1) used a dataset comprising 20 river flow time series from the Iranian Central Plateau River Basin. The selection of the best distribution for each station was based on the values of the lowest residual sum of squares (RSS). The results showed that the L-moment method demonstrated adequate accuracy for both gauged and ungauged site frequency analysis. Furthermore,

Pearson Type III distributions emerged as the best-fit regional model for the Iranian Central Plateau River Basin. (Ahmad, M. Yasin, M. Fawad, and A. Saghir, 2017) studied regional frequency analysis of low flows using L-moments for the Indus basin in Pakistan. They separated the region into two regions; Generalized Normal (GNO) was Region-I's most appropriate probability distribution, while (GPA) was for Region II.

Recently, other approaches have been applied to investigate and analyze regional frequency analysis for low-flow series. (J. Ouarda and C. Shu, 2008) introduced single and ensemble artificial neural networks (ANNs) to obtain improved regional low-flow estimates at ungauged sites. Sang Ug Kim and Kil Seong Lee (2010) used Bayesian regression and prediction in unrestricted catches in Korea and the ordinary small squares method for regional low-flow frequency. Only (Sawaske and Freyberg, 2014) focused on identifying and calculating indicators representing annual low-flow conditions and the primary form of recession. Their results showed that during the past forty to eighty years, there have been widespread trends of high base flow stagnation rates and decreasing low annual flow conditions across the region.

Staudinger and Seibert (2014) assessed the relative significance of current hydrological conditions and weather during the prediction period. Their findings revealed that the maximum detectable effects of initial conditions varied from 50 days to at least one year. Du et al. (2015) enhanced the nonstationary return period and risk characterization under ENE interpretation by utilizing common meteorological variables in nonstationary frequency analysis. Christian Charron (2015) conducted regional low-flow frequency analysis by incorporating a recession parameter derived from a nonlinear reservoir model, defining 29 recession characteristics that were used as predictors in regional models.

2.2 Applied Research in Turkey

Many studies have also been carried out over the past two decades in Turkey. However, because most of the 26 basins (D. Aydogan 2014) do not have enough sites, and most of those hosting a site have short records, the length of the time series is insufficient to be well evaluated. Both on-site RFFAs (received from the sites) and synthetic methods are employed in estimating the flow rates. Synthetic methods were used in Turkey due to the lack of information on the flows. With the increase in the length of data collected from flow sites, new methods have been combined with statistical analyses to estimate flow values with many non-transcendent possibilities.

Saf (2008) examined the annual flood peak series recorded at 48 stream-gauging stations in the basins of Turkey's West Mediterranean region. She categorized the data into three homogeneous subregions using the t-test and the Dalrymple homogeneity test. In a subsequent study, Saf B (2009) aimed to determine regional probability distributions for the annual maximum flood data observed at 45 streamflow gauging sites in the Kucuk and Buyuk Menderes River Basins in Turkey, employing

the index flood procedure. According to the L-moment goodness-of-fit statistic criterion, the GEV distribution was identified as the best-fit distribution for the region.

Seckin et al. (2011) applied the index flood procedure coupled with the L-moments method to the annual flood peaks data taken at all stream gauge stations in Turkey having at least 15-year-long records. Depending on this study, GEV and Wakeby are selected as the best-fit distributions, whose parameters are computed by the L-moments method, which was adequate for predicting quantile estimates. In (2013), Dikbas et al. applied a study to define Homogeneous Regions for Streamflow Processes in Turkey using a k-Means clustering method. The k-Means method is recommended for identifying hydrologically homogeneous regions in regional frequency analysis.

Aydogan, et al. (2016) used the L-moments method to conduct a regional flood frequency analysis of the Oruh basin. Because of its size, the Çoruh basin was divided into four sub-regions. Omer Levend Asikoglu (2017) investigated Turkish rivers' parental flood frequency distribution. The study collected annual peak series from 268 Turkish rivers, and a database of L-Moment ratios was constructed. The results of a graphical inspection of the dataset show GEV distribution as a potential parent PD of the floods in Turkey. Cetin et al. (2018) applied a frequency analysis of low flows in intermittent and nonintermittent rivers from hydrological basins in Turkey. LN3 generally aligns well with low flows, serving as the best fit among the selected probability distribution functions in three out of the four hydrological basins. In contrast, W3 only fits low flows in one basin according to this study.

2.3 A Comparison of Unbiased and Plotting-Position Estimators of L Moments

In the field of regional frequency analysis, the comparison between unbiased estimators and plotting-position estimators has been a subject of considerable research. Hosking & Wallis (1995), in his study published in Water Resources Research, advocates for the use of unbiased estimators in general applications, highlighting their accuracy and reliability. However, the authors also acknowledge that plotting-position estimators can be beneficial in certain contexts, especially when estimating extreme quantiles, which are crucial in hydrological applications. On the other hand, Hirsch & Stedinger (1987) illustrates that plotting positions that are unbiased when used with uncensored samples can become biased when applied to a combination of historical and systematic data. This finding highlights the importance of understanding the context in which these estimators are used. Kim (2007), in his study, focuses on the impact of five different plotting positions within the Probability Weighted Moments (PWM) method. His findings indicate that the Landwehr plotting position generally results in smaller biases when estimating both location and scale parameters compared to other plotting positions. This result suggests that while unbiased estimators offer overall robustness, specific plotting positions like Landwehr may reduce bias in certain estimations, further enhancing accuracy in regional analyses.

Recently, Muangsuwan et al (2017) investigated and compared between the MLE and PWM methods. The results indicated that for small sample sizes, the modified plotting position method exhibited the lowest bias value and root mean square error (RMSE) among the three methods. This suggests that it is more reliable for estimating parameters when data is limited. Conversely, for large sample sizes, the MLE method outperformed the others, showing the lowest bias value and RMSE. This indicates that MLE is more effective when a larger dataset is available.

3. MATERIAL AND METHOD

3.1 Material

Turkey is located in the northern hemisphere, between Europe and Asia, on the Anatolian Plateau and the Thrace Peninsula. Turkey's land is roughly shaped like a rectangle, with 36-42° north parallels and 26-45° east meridians. The Mediterranean Sea, the Black Sea, and the Aegean Sea surround the country. In general, the country has four different climate types. The Black Sea climate is rainy all year in the north. The Mediterranean climate is hot and dry in Summer and warm and rainy in winter in the west and south. In Central Anatolia and South-eastern Anatolia, a semi-arid climate exists, and in Eastern Anatolia, the continental weather is very cold in winter and rainy in summer.

Turkey, in general, is divided into 26 major river basins for hydrological studies. The basins list and the map showing the mainstream basins are in Table 3.1 depending on the observational years of the Electricity Works Survey Administration (EIEI) and State Water Works (DSI), according to the basin numbers. The average annual flow in the basins is 186 BCM. The Firat-Dicle Rivers Basins are Turkey's largest in terms of surface area and water potential, accounting for 28.4% of the country's total water potential. The average annual precipitation in Turkey is approximately 400 mm.

The total surface area of Turkey is 780 000 km^2 (78 million hectares). Turkey has more than 120 natural lakes, including small lakes in the mountains. In addition to the natural lakes, there are a total of 555 dam lakes in Turkey, 544 of which were built and taken into operation by the DSI (Devlet Su İşleri), and other institutions constructed. When the dam and natural lakes are removed, the remaining area is 769,600 km^2. The average altitude of Turkey is 1132 m. In the east, the altitude reaches 4000 m, and the altitude of the plains reaches 2000 m. Semi-arid climate characteristics can be seen in Turkey.

On the other hand, due to Turkey's geographical location and geomorphological structure, climate characteristics change rapidly over short distances. Temperature, precipitation, and winds vary depending on climatic characteristics. The six-degree latitude difference between the north and south also plays an important role in temperature variation. The climate in the interior is steppe. Depending on the surface structure of the ground, the precipitation falling to the ground partially passes into the surface flow and channel flow, forming streams and rivers. Every river has a basin where it collects water. Turkey is divided into 26 hydrological basins. Out of the 26 basins determined, 15 are river basins, 7 are mixed basins consisting of generally smaller rivers with different flow rates, and 4 are closed basins that do not discharge into the sea. Figure 3.1 shows the geographic distribution of the basins in Turkey.

Table 3.1 Basins in Turkey and their characters

#	Name of the Basin	Catchment Area (km^2)	Mean Annual discharge (billion m^3)	Contribution to total discharge (%)
1	(21)(26) Firat - Dicle River Basin	184.918	52.94	28.4
2	(22) East Black Sea Basin	24.077	14.90	8.0
3	(17) East Mediterranean Basin	22.048	11.07	6.0
4	(09) Antalya Basin	19.577	11.06	5.9
5	(13) West Black Sea Basin	29.598	9.93	5.3
6	(08) West Mediterranean Basin	20.953	8.93	4.8
7	(02) Marmara Basin	24.100	8.33	4.5
8	(18) Seyhan River Basin	20.450	8.01	4.3
9	(20) Ceyhan River Basin	21.982	7.18	3.9
10	(15) Kizilirmak River Basin	78.180	6.48	3.5
11	(12) Sakarya River Basin	58.160	6.40	3.4
12	(23) Coruh River Basin	19.872	6.30	3.4
13	(14) Yesilirmak River Basin	36.114	5.80	3.1
14	(03) Susurluk River Basin	22.399	5.43	2.9
15	(24) Aras River Basin	27.548	4.63	2.5
16	(16) Konya Closed Basin	53.850	4.52	2.4
17	(07) Buyuk Menderes River Basin	24.976	3.03	1.6
18	(25) Van Lake Basin	19.405	2.39	1.3
19	(04) North Aegean Basin	10.003	2.90	1.1
20	(05) Gediz River Basin	18.000	1.95	1.1
21	(01) Meric - Ergene River Basin	14.560	1.33	0.7
22	(06) Kucuk Menderes River Basin	6.907	1.19	0.6
23	(19) Asi River Basin	7.796	1.17	0.6
24	(10) Burdur Lake Basin	6374	0.50	0.3
25	(11) Akarcay Basin	7.605	0.49	0.3
	Total	**779,452**	**186.86**	**100**

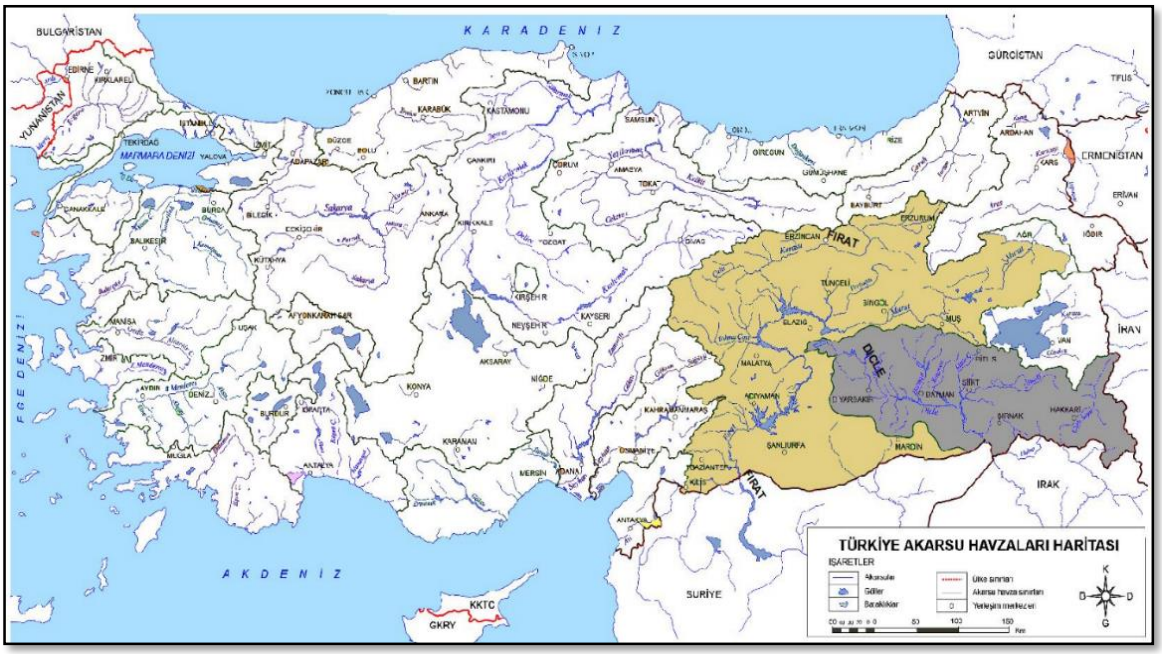

Figure 3.1 Basins in Turkey (CografyaHarita, 2017)

3.2 Method

3.2.1 Regional frequency analysis

Since all stations in a basin do not have the same climatic conditions and geographical features, it is incorrect to choose the same frequency distribution for all records. The hydrological data must be long enough for frequency analysis to give accurate and sensitive results, but the available data on a station-by-station basis is often insufficient. At the same time, since similar stations around any station have measured the available hydrological data, many datasets are likely to have the same statistical characteristics. The expectation that more accurate results will be achieved by examining the data at the relevant stations has created a new analysis technique, regional frequency analysis. Another important aspect of regional frequency analysis is that the stations considered in a region do not have to be geographically adjacent or close (Şorman and Okur, 2000).

In this study, regional frequency analysis was used. For regional analysis, the region is divided into homogeneous sub-regions if stations with similar statistical characteristics are considered. Thus, a general frequency distribution is obtained for each homogeneous region in droughts forecasts.

The index flood procedure (a regional frequency analysis method) is based on the principle that the frequency distributions in the stations that are accepted as in the region are the same except for a certain scale factor belonging to that station. As mentioned earlier, homogeneous basins belonging to stations considered regions do not need to be geographically contiguous because geographic proximity does not require station frequency distribution to be the same. This provides great advantages for regional frequency analysis; in addition, stations can be considered in the same region without being in close geographic proximity. Another advantage of this situation is that it reduces the correlation between stations.

3.2.2 Delineation of Homogeneous Regions

Hosking and Wallis (1997) indicated that it is possible to estimate the degree of coherence in a group of stations and assess when these can be treated as a homogeneous region. In particular, the measure of heterogeneity, H, compares the variability of the L-moments samples of a group of stations that make up the region with the expected one obtained from simulation techniques. The region is declared heterogeneous if the value of H is sufficiently high. According to Hosking and Wallis (1997), it is "acceptably homogeneous" if $H < 1$, "possibly heterogeneous" if $1 < H < 2$, and "heterogeneous" if $H > 2$. Negative values indicate that the sample L-cv dispersion is less than expected in a homogeneous region with independent local distributions, implying a positive relationship between stations and their cause. The used heterogeneity test is based on the L-coefficient of variation (L-cv). This test uses the weighted variance of the L-cv of each of the stations according to the statistical:

$$V = \left(\frac{\sum_{i=1}^{N} n_i \left(t^{(i)} - t^R\right)^2}{\sum_{i=1}^{N} n_i} \right)^{0,5} \quad (3.1)$$

The measure of heterogeneity H is defined as:

$$H = \frac{V - \mu_V}{\sigma_V} \quad (3.2)$$

3.2.3 Discordance Measure

Hosking and Wallis (1997) explained that if there are N sites in a group of stations, the objective is to identify those extremely discordant with the group. Discordance D_i is measured in terms of the L-moments of the site data, which is defined statistically for a site i in a dataset with N sites by:

$$D_i = \frac{1}{3} N (U_i - \overline{U})^T A^{-1} (U_i - \overline{U}) \quad (3.3)$$

A site is considered discordant if $D_i > 3$. All individual stations that exceed this threshold must be subjected to a thorough quality analysis to find the possible causes that differentiate them from the rest of the group.

3.2.4 L-Moments Approach

Hosking and Wallis (1997) state that there is an alternative method of L-moments for describing the shapes of probability distributions by making modifications to Greenwood et al.'s probability-weighted moments (PWMs) (1979). Probability-weighted moments are defined as:

$$\beta r = E \{X[F(X)]r\} \quad (3.4)$$

Where:

F = F(x) = cumulative distribution function for x (CDF),

x (F) =inverse CDF of x evaluated at the probability F,

r =0,1, 2,… nonnegative integer. When r =0, β_0 is equal to the mean of the distribution.

For any distribution, the L-moment λ_r is related to the r_{th} PWM (Hosking 1990) through:

$$l_{r+1} = \sum_{k=0}^{r} p_{r,k}^{*} \, b_k \quad (3.5)$$

Where:

$$p^*_{r,k} = (-1)^{r-k}\binom{r}{k}\binom{r+k}{k} \quad (3.6)$$

$$b_r = n^{-1}\sum_{j=1}^{n}\frac{(j-1)(j-2)\ldots\ldots(j-r)}{(n-1)(n-2)\ldots\ldots(n-r)}x_j \quad (3.7)$$

For example, the first five L-moments:

$l_1 = b_1$

$l_2 = 2b_1 - b_0$

$l_3 = 6b_2 - 6b_1 + b_0$

$l_4 = 20b_3 - 30b_2 + 12b_1 - b_0$

$l_5 = 70b4 - 140b3 + 90b2 - 20b1 + b0$ (3.8)

Hosking (1990) defined L-moment ratios as:

- L-coefficient of variation, L-cv (τ_1) = l_2/ l_1
- L-coefficient of skewness, L-skew (τ_3) = l_3/ l_2
- L-coefficient of kurtosis, L-kurtosis (τ_4) = l_4/ l_2

L-moments, like ordinary product moments, summarize the properties by finding theoretical probability distributions to model the observed samples, according to (Zafirakou-Koulouris et al., 1998). The measures of distributional location (mean), scale (variance), skewness (shape), and kurtosis are done for both moments types (peaking). The authors state that L-moments have several advantages over regular product moments, particularly for environmental datasets, because of the following:

1. Regardless of the probability distribution from which the observations are derived, L-moment ratio estimators of location, scale, and shape are nearly unbiased (Hosking, 1990).
2. L-moment ratio estimators such as L-cv, L-skewness, and L-kurtosis, especially for highly skewed samples, can have lower bias than conventional product moment ratios.
3. Unlike the ordinary product moment ratio estimators of cv and skewness, the L-moment ratio estimators of L-cv and L-skewness do not have bounds dependent on sample size.
4. Product moment estimators, square or cube values of the observations, are less sensitive to the largest observations in a sample than L-moment estimators, which are linear combinations of the data.

5. L-moment ratio diagrams excel at identifying the distributional features of severely skewed data, but standard product moment diagrams are nearly useless (Vogel and Fennessey, 1993).

3.2.5 A Comparison between Unbiased and Plotting-Position Estimators

Given an ordered sample of size n, $x_{1:n} \leq x_{2:n} \leq \ldots \leq x_{n:n}$ There are two established ways of estimating the probability-weighted moments and L-moments of the distribution from which the sample was drawn. Considering the probability-weighted moment αr firstly, Landwehr et al. [1979a] used the unbiased estimator:

$$\alpha_r = n^{-1} \sum_{j=1}^{n} \frac{(n-j)(n-j-1)\ldots(n-j-r+1)}{(n-1)(n-2)\ldots(n-r)} x_{j:n} \quad (3.9)$$

Landwehr et al. [1979b] preferred the estimator:

$$\bar{\alpha}_r = n^{-1} \sum_{j=1}^{n} (1 - P_{j,n})^r x_{j,n} \quad (3.10)$$

With $P_{j,n}$= (J - 0.35)/n. This estimator is called a "plotting-position estimator" because $P_{j,n}$is a plotting position, a distribution-free estimator of the no-exceedance probability of $x_{j,n}$.

Estimators can similarly be obtained for the probability-weighted moment's βr and L-moments ratios. For L-moments, unbiased estimators are given by:

$$l_{r+1} = (-1)^r \sum_{k=0}^{r} p^*_{r,k}\, b_k \quad (3.11)$$

The analogous estimators of L-moment ratios are:

$\tau_r = l_r / l_2$ (3.12)

These estimators are not unbiased, but based on their construction, it is convenient to refer to them as "unbiased" estimators. Plotting-position estimators of L-moments and L-moment ratios are given by:

$$\bar{\lambda}_{r+1} = (-1)^r \sum_{k=0}^{r} p^*_{r,k} \bar{\alpha}_k \quad (3.13)$$

$$\bar{\tau}_r = \frac{\bar{\lambda}_r}{\bar{\lambda}_2} \quad (3.14)$$

The plotting position and unbiased estimators are equivalent in large samples; the difference between them is a random number of orders n^{-1}. Thus, the question of what the preferred is in

practice depends on the characteristics of the estimators in small and moderate samples. Landware et al. (1979) recommended planning probability-weighted moments because, when they were used to fit the Wakeby distribution, they gave more accurate estimates of the quantities in the upper tail. Hosking et al. [1985b] and Hosking and Wallis [1987] came to the same conclusion regarding the generalized maximum value and Pareto distributions, respectively. These authors were principally concerned with "flood-like" distributions having $\frac{\bar{\lambda}_2}{\bar{\lambda}_1}$ (the L moment analogue of the usual coincident of variation) and both in the approximate range of 0.1 to 0.3.

L-moments have recently found other applications, including summary statistics of data samples [Hosking, 1990], for determining the appropriate distribution that fits the dataset (Chowdhury et al., 1991) and (Hosking and Wallis, 1993). Also, for fitting distributions to data, such as monthly rainfall totals and, more importantly, for the deviation from the maximum annual flood data [Guttman et al., 1993]. Moreover, the advantages of plotting positions estimators over the unbiased estimates for quantitative estimation are slight, except in some regional frequency analysis. Therefore, it is concluded that for general use, unbiased estimators are preferred over estimating parking estimators. The only exception is the estimation of severe upper-tail quantities in regional frequency analysis; hence, the plotting position sometimes outperforms the unbiased estimators.

3.2.6 Monte Carlo Simulation

Monte Carlo simulation is used to evaluate the accuracy of recurrence prediction. This method is a technique grounded in probability theory. It involves simulating and solving an experiment or physical event by employing statistical and mathematical techniques that utilize random numbers repeatedly. The inter-station variation in the population L-moment ratios of the simulated region must always be smaller than that of the sample L-moment ratios of the actual data. That is because the sample variability causes the sample L-moment ratios to spread over a wider area than the appropriate population L-moment ratios.

For this reason, L-cv values are modified in the input file of the simulation program before being used. The range of L- cv values at the stations is divided into two parts. In contrast, the regional weighted average values remain constant, ranked in ascending order, and the middle value is the regional weighted average value. On the way up, this value is reduced by the difference between the maximum and minimum values. Thus, new L- cv values are obtained. These values are used in the XSIM program (Hosking and Wallis, 1997).

3.2.7 Return Period, Probability, and Plotting Position

Droughts peaks do not occur with any fixed pattern in time or magnitude. The intervals between Droughts differ. The average inter-event period between droughts episodes is the return period (Cunnane, 1989). Droughts, on the other hand, have long return times. There may be no

mention of probability in the specification of the return period. On the other hand, a link between the likelihood of a droughts and its return period can be justified. Once every T years, a given droughts q with a return duration T may be exceeded. The cumulative probability of non-exceedance, $F(Q_T)$ is given by Eq 3.15.

$$F(Q_T) = 1 - p(Q_T \leq q) = p(Q_T \geq q) = \frac{1}{T} \tag{3.15}$$

Equation 3.15 is the basis for estimating the magnitude of an extremely low event. With Q_T given, it returns period T. Substituting F (Q_T) = 1/T in a known statistical distribution function, one can solve for the magnitude of Q_T. Often, the data are plotted on probability paper to check whether they follow a particular distribution, to detect errors, and to check for outliers.

Probability plots require an initial estimate of the probability of non-exceedance F = (F (Q_T)), which is called a "plotting position." Plotting positions are also used to estimate parameters using the probability-weighted moments (PWM) method. A plotting-position formula that is used in this thesis is given by Hosking (1990):

$$F = \frac{i-0.35}{N}, i = 1, 2, \ldots\ldots, N \tag{3.16}$$

where N is the sample size, and i is the ascending order of the observations. Eq 3.15 is employed in the PWM approach because it is thought to yield acceptable results for some common three-parameter distributions (Hosking, 1990).

3.2.8 L-Moment Diagrams

For various assumed distributions, L-moment diagrams compare sample estimates of the L moment ratios L-cv, L-skew, and L-kurtosis with their population counterparts. L-moment diagrams have an advantage over other goodness-of-fit procedures; they allow the comparison of the fit of several distributions to multiple samples of data using a single graphical tool. Another advantage of L-moment diagrams over ordinary product moment diagrams is that, unlike ordinary product moment ratios, which are strongly biased for all probability distributions, L-moment ratios are nearly unbiased for all probability distributions (Vogel and Fenness, 1993). The theoretical relationships among L-skew and L-kurtosis for the Pearson type III (P3), GEV, three-parameter lognormal (LN3), three-parameter Weibull (W3), and the lower bound of a Wakeby distribution (WLB) are shown as curves in Figure 3.2, are obtained from the polynomial approximations given in Hosking (1991) and Stedinger et al. (1993).

Only Hosking (1990) and Stedinger (1990) provide exact relationships between L-cv and L-skewness for two possible distributional parameters (1993). Polynomial approximations are done to the theoretical correlations between L-cv (2) and L-skew (3) for the two-parameter lognormal (LN2),

Weibull (W2), and Gamma (GAM), and generalized Pareto distributions to make the creation of L-moment diagrams easier in future investigations (GP). It is not intended to use detailed analytical calculations; instead, the exact equations given by Hosking (1990) and Stedinger (1993) are used. The approximations are summarized in Table 3.2.

Table 3.2 Type of distribution

Distribution	**Code**	**Number of parameters**	**Parameters**	**F(x), x(F)**
Exponential	EXP	2	ξ, α	$F = 1 - \exp\left\{-\frac{x-\xi}{\alpha}\right\}$ $x = \xi - \alpha \log(1 - F)$
Gamma	GAM	2	α, β	$F = G(\varkappa/\beta, \alpha)$ not explicitly defined
Generalized extreme value	GEV	3	ξ, α, k	$F = \exp[-\{1 - K(\varkappa - \xi)/\alpha\}^{1-\kappa}]$ $x = \xi + \alpha\{1 - (-\log F)^K\}/k$
Generalized logistic	GLO	3	ξ, α, k	$F = 1/[1 + \{1 - k(x - \xi)/\alpha\}^{1/K}]$ $x = \xi + \alpha[1 - \{(1 - F)/F\}^K]/k$
Generalized Normal	GNO	3	ξ, α, k	$F = \Phi[-k^{-1} \log\{1 - k(x - \xi)/\alpha\}]$ x(F) not explicitly defined
Generalized Pareto	GPA	3	ξ, α, k	$F = 1 - \{1 - k(x - \xi)/\alpha\}^{1/k}$ $x = \xi + \alpha\{1 - (1 - F)^k\}/k$
Gumbel	GUM	2	ξ, α	$F = \exp[-\exp\{-(x - \xi)/\alpha\}]$ $x = +\alpha \log(-\log F)$
Kappa	KAP	4	ξ, α, k, h	$F = [1 - h\{1 - k(x - \xi)/\alpha\}^{1/K}]^{1/h}$ $x = \xi + \alpha[1 - \{(1 - F)^h/h\}^K]/k$
Normal	NOR	2	μ, σ	$F = \Phi\left\{\frac{x - \mu}{\sigma}\right\}$ x(F) not explicitly defined
Pearson type III	PE3	3	μ, σ, γ	$F = G\left(\frac{x - \mu + \frac{2\sigma}{\gamma}}{\left\lvert\frac{\sigma\gamma}{2}\right\rvert \cdot \frac{4}{\gamma}}\right)$ x(F) not explicitly defined
Wakeby	WAK	5	ξ, α, β, γ, δ	$\emptyset(\varkappa) = (2\pi)^{-\frac{1}{2}} \int_{-\infty}^{x} \exp\left(\frac{-t^2}{2}\right) dt$ $G(\varkappa, \alpha) = \{\tau(\infty)\}^{-1} \int_0^{\varkappa} T^{\alpha-1} e^{-t} dt$

3.2.9 Identification of the regional distribution function

Once it has been verified that the station makes up a homogeneous region, it is necessary to identify the underlying distribution function for the variable under consideration. The hypothesis

underlying homogeneity is that the frequency distributions that follow the data from the different locations are the same except for a specific scale factor for each location represented by the mean data from each location. This is the index avenue procedure (Dalrymple, 1960; Hosking and Wallis, 1997).

The L-moment methodology provides several possible distribution functions by matching the L-moments of the data for each location with the corresponding parameters of the distribution. To identify the best distribution function in the region, the five most common distribution functions of three parameters have been considered in the analysis of frequencies of extreme values: GPAR (Generalized Pareto), P-III (Pearson type III), LOGN (Log-normal of three parameters), GLOG (Generalized Logistics), and GEV (Generalized for Extreme Values). The diagram of the quotients of L-moments is shown in (Figure 3.2)

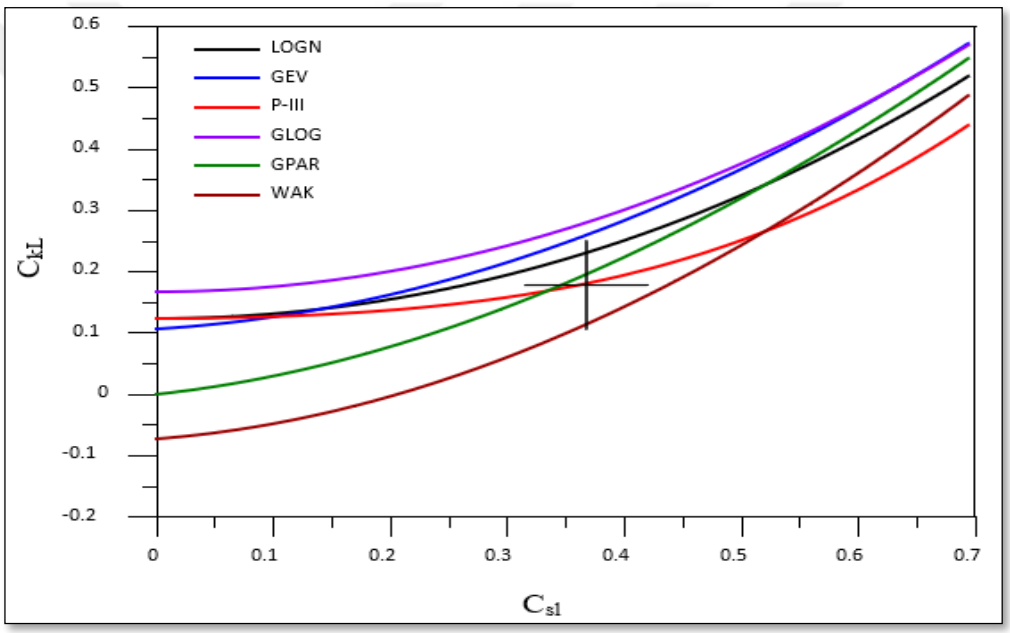

Figure 3.2 C_{kl}- C_{sl} diagram and the curves of distributions.

3.2.10 Z score calculation

Hosking and Wallis (1993, 1997) developed the Z_{dist} statistic for the parameter distributions, which quantifies the goodness of fit of the candidate distribution function to the regional data based on the C_{kL} coefficients of the distribution and the average regional C_{kL} of the observed data.

$$Z_{Dist} = \frac{t_4^R - t_4^{Dist}}{\sigma_4} \tag{3.17}$$

If $Z_{dist} \leq 1.64$ for a specific distribution function, the distribution is considered acceptable to represent the data for the region. But due to the spatial correlation between data from different stations, satisfying the normality hypothesis for the associated Z statistic (which requires the region

to be homogeneous) is impossible. Therefore, Z_{dist} should be seen as a rough indication and incapable of accurately identifying the most descriptive distribution function.

3.2.11 Estimation of extreme quantiles associated with interest return periods

The instantaneous annual maximum flow quantiles, associated with the different return periods T, are estimated from each acceptable regional distribution function by the index flood procedure. In this procedure, it is assumed that the frequency distribution functions of all the stations that make up a homogeneous region are identical, except for a local scale factor known as the index flood. For each of the stations within each homogeneous region, the estimates of the quantiles are calculated according to the following expression:

$$Qi\ (F) = \mu_i .\ q(F) \tag{3.18}$$

Where:

Qi (F) = estimate of the quantiles associated with the station (i), for a probability of non-exceedance $F\mu_i$ equal to the index flood calculated by averaging the annual series of maximum instantaneous flows at each station. Qi (F) = regional curve (dimensionless frequency or growth curve), common to all regional stations.

The precision of the estimated quantiles for each T is evaluated using Monte Carlo simulations, obtaining the relative mean square error (RMSE) and the confidence limits associated with a certain degree of significance. The distribution with the lowest RMSE is the most robust and has the best predictive capacity.

4. RESULTS AND DISCUSSIONS

The next four stages comprise the regional frequency analysis based on the Hosking and Wallis index flood procedure, with its parameters determined using L-moments:

a. Filtering the series of observations.
b. Identifying homogeneous regions.
c. Choosing the frequency distribution function.
d. Estimating extreme quantiles for interest return periods.

4.1Firat basin stations

The dataset consists of annual records of minimum streamflow at 33 sites throughout the Firat River. This data was available from the General Directorate of Electrical Power Resources Survey and Development Administration (EIE) from 1957 to 2007. The study duration depended on the station location. The available data ranged from 16 to 46 years, with an average of 31 years of records per site. Table 4.1 shows the station names and their characteristics. Figure 4.1 shows the geographical distribution of stations in the basin.

Table 4.1 Used Stations in Firat Basin

No	Station Name	Area (km^2)	Elevation	Q_{mean}	(E)	(N)
2103	Firat- Karakaya	63874	688	176.2	39.1	38.2
2115	Goksu river - Malpinar	3990	397	17.07	38.2	37.5
2119	Kemab strait	10356	1123	22.54	39.4	39.7
2122	Murat river - Tutak	5882	1552	7.08	42.8	39.5
2123	Cinarkoy	864	560	8.8	41.3	37.2
2124	Tohmasuyu - yazkoy	1336	1100	5.8	37.4	38.7
2125	Sultan Water - Sucati	450	995	1.75	38.0	38.2
2131	Beyderesi - Kilayik	278	925	0.46	38.2	38.3
2133	Munzur - Melekbahce	3285	875	26.75	39.5	39.0
2135	Bulam - Fatopasa	155	1252	1.67	37.4	37.1
2140	Dutluca	92654	386	259.1	38.2	38.0
2141	Peri Water - Korudibi	3604	1100	11.96	40.1	39.2
2145	Tohma Water - Hisarcik	5822	935	14.98	37.7	38.5
2147	Munzur- Dedikusagi	808	1250	13.74	39.3	39.3
2149	Munzur - Miskisag	1622	925	19.32	39.5	39.1
2151	Demirkapi	8186	1355	10.47	40.2	39.6
2154	Karasu - Asagikagdaric	2886	1675	2.63	40.8	39.9
2155	Tercan kop	2144	1415	2.95	40.4	39.8
2156	Bagistas	15562	865	64.89	38.5	39.4
2157	Karasu - Karakopru	2098	1250	1.77	41.5	38.8
2158	Abdurahmanpasa	1577	1310	2.5	41.5	39.1
2159	Cam Stream	1036	525	0.45	39.1	37.7

Table 4.1 (Continued)

2164	Goynuk- Cayagzi	2232	998	1.84	40.6	38.8
2165	Zerkan water - hocakoy	490	445	0.07	40.5	37.1
2166	Peri Water - Logmar	5446	842	9.42	39.8	38.9
2167	Calti Water	4288	890	2.59	38.3	39.3
2168	Dumlu Stream	52	2000	0.14	41.4	40.1
2171	Uludere	411	118	0.03	37.9	38.9
2172	Pulumur Stream	1374	890	8.25	39.6	39.1
2173	Sultan Water	186	935	0.72	38.0	38.2
2174	Murat river - Akkonak	17435	1285	21.33	41.5	39.0
2176	Mutu strait	94	1225	1	39.9	39.6
2177	Hinis stream - Adivar	2995	1452	5.38	42.2	39.2

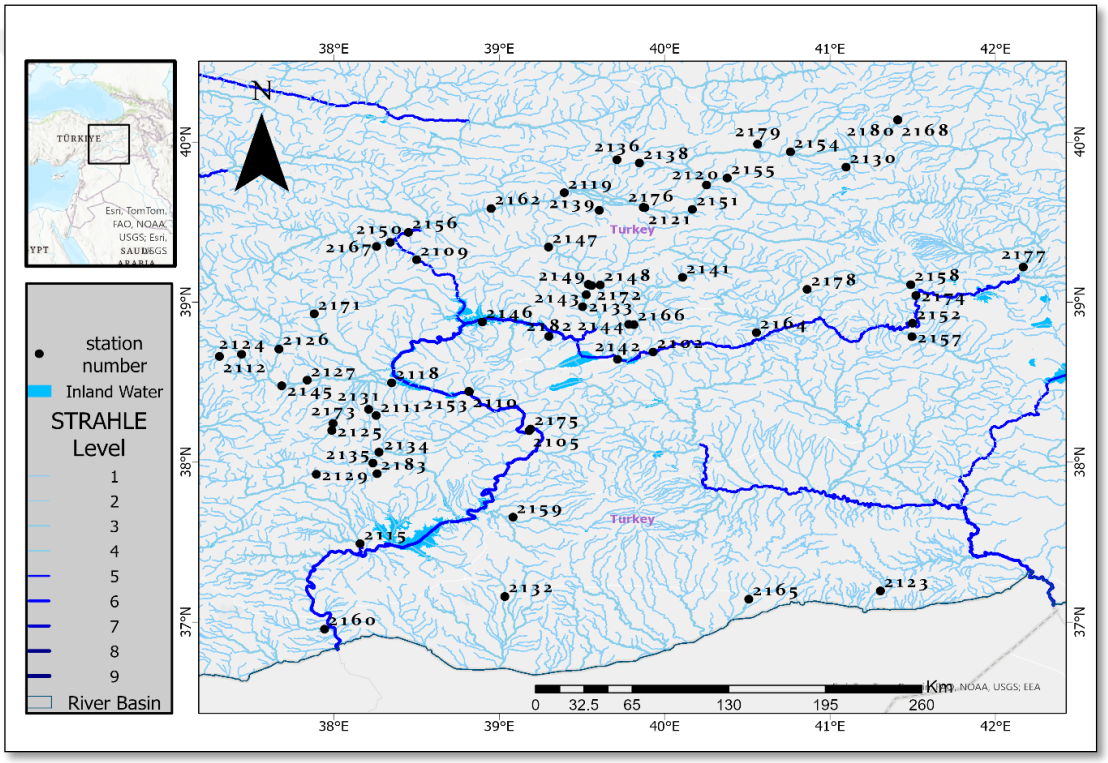

Figure 4.1 Geographical distribution of stations in the Firat basin.

A regional frequency of low flow analysis utilizing the index flood procedure paired with the L-moments approach is applied to the Firat rivers basin in Turkey using the yearly low flow peak series of 33 stream-gauging stations. L-Moment Values were calculated using both plotting position estimators and unbiased estimators by Excel. Figure 4.2 depicts the association between τ_1 and τ_3 for all stations.

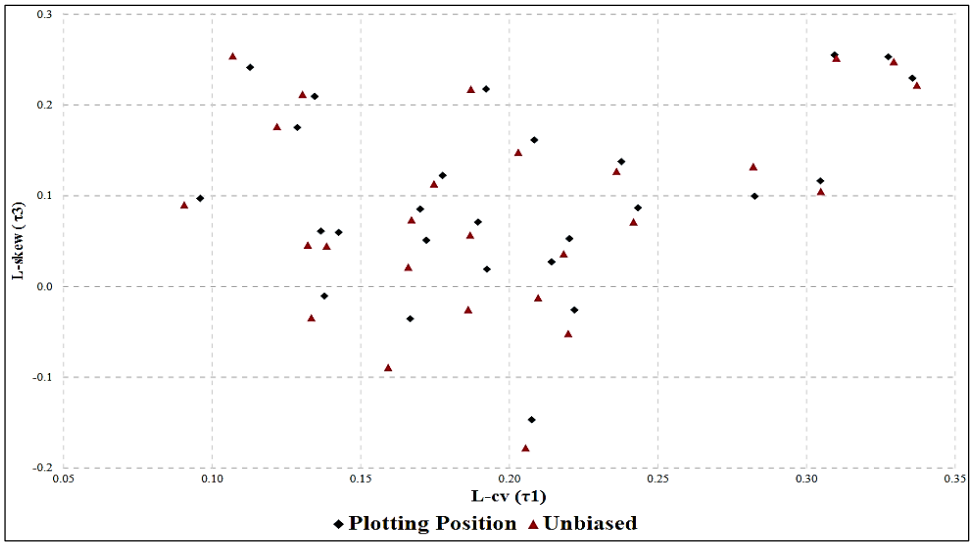

Figure 4.2 The relationship between τ_1 and τ_3 for all station in Firat Basin

The heterogeneity measures, H (1), H (2), and H (3), were estimated using 500 simulations utilizing data from 33 sites. based on unbiased estimators H values are (21.17), (9.01), and (7.86). while depending on Plotting Position Estimators H Values are (14.65), (3.07), and (0.37). The high values of L-skew and L-kurt (0.653 and 0.65, respectively) in the Firat stations generated severe discordancy and illustrated the impact of an outlier on homogeneity.

Because H (1), H (2), and H (3) are all greater than 3.0, these numbers imply that the Firat River Basin is a heterogenous zone (Hosking and Wallis 1997). To define the homogeneous region, the region must be divided into three sub-regions. Stations with D values greater than critical value are disqualified. Based on the results of all Firat basin stations, 26 stations were included in this study, where 7 stations have been removed based on unbiased estimator and Plotting Position estimator. Figure 4.3 depicts the distribution of stations depending on τ_1 and τ_3 values.

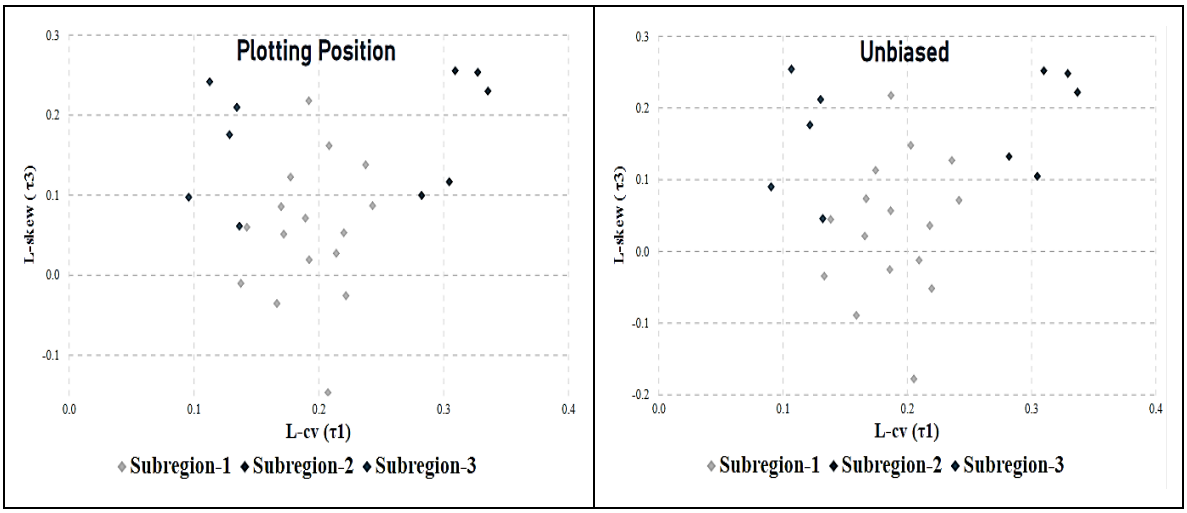

Figure 4.3 The relationship between τ1 and τ3 for sub regions in Firat Basin.

Table 4.2 shows the values of τ_1(L-cv), τ_3 (L-skew), and the discordancy measure Di for 32 stations. All calculations were computed for the subregion using Hosking's Fortran computer software (1991). The L-cv and L-skew values estimated from the recorded sample series of these 32 stations are based on the plotting position estimators. The results show that all Di values are less than the crucial value.

Table 4.2 L-Moments values for the Firat basin depending on plotting position estimators.

Sub Region	Station	Record length	Mean	τ_1	τ_3	τ_4	τ_5	D_i	D_c
First Subregion	2103	18	176.3	0.193	0.019	0.220	-0.018	0.34	3
	2115	42	14.110	0.220	0.052	0.156	0.012	0.28	
	2124	46	6.133	0.208	-0.147	0.231	0.031	2.4	
	2133	40	26.230	0.143	0.059	0.165	0.008	1.1	
	2135	43	1.460	0.178	0.122	0.120	0.031	0.76	
	2140	18	259.06	0.209	0.161	0.205	0.051	0.95	
	2145	45	13.042	0.170	0.085	0.145	0.053	0.46	
	2151	43	11.006	0.190	0.071	0.104	0.008	0.74	
	2154	39	2.673	0.238	0.137	0.126	0.061	1	
	2155	19	2.945	0.167	-0.036	0.274	-0.042	1.53	
	2157	39	1.805	0.243	0.086	0.149	0.000	0.92	
	2158	38	2.333	0.138	-0.011	0.205	0.066	1.24	
	2164	38	1.840	0.222	-0.026	0.127	0.037	0.95	
	2167	22	2.589	0.172	0.051	0.158	-0.007	0.26	
	2174	20	21.331	0.214	0.027	0.131	0.000	0.41	
	2177	22	5.383	0.192	0.217	0.252	0.143	2.65	
	Regional	_	**34.26**	**0.194**	**0.049**	**0.165**	**0.027**	_	
Second Subregion	2125	16	1.749	0.310	0.255	0.229	0.058	0.94	1.33
	2131	46	0.386	0.305	0.116	0.089	0.088	1.12	
	2166	38	9.421	0.283	0.099	0.046	0.061	1.14	
	2168	25	0.138	0.336	0.229	0.199	0.051	1.27	
	2171	16	0.033	0.328	0.253	0.238	0.218	0.53	
	Regional	_	**2.345**	**0.308**	**0.162**	**0.129**	**0.095**	_	
Third Subregion	2119	38	22.377	0.137	0.061	0.163	0.077	1.02	1.33
	2147	33	13.494	0.113	0.241	0.163	0.004	0.74	
	2149	41	18.228	0.135	0.209	0.048	-0.016	1.26	
	2156	39	66.131	0.096	0.097	0.224	0.021	1.25	
	2172	26	8.245	0.129	0.175	0.181	0.031	0.74	
	Regional	_	**25.7**	**0.122**	**0.153**	**0.153**	**0.024**	_	

Table 4.3 shows the values of τ_1(L-cv), τ_3 (L-skew), and the discordancy measure Di for 30 stations. All calculations were computed for the subregion using Hosking's Fortran computer software (1991). The L-cv and L-skew values estimated from the recorded sample series of these 30 stations are based on an unbiased estimator. The results show also that all Di values are less than the crucial value.

Table 4.3 L-Moment Values for the Firat basin depending on unbiased estimators.

Sub Region	Station	Record length	Mean	τ_1	τ_3	τ_4	τ_5	D_i	D_c
First Subregion	2103	18	176.3	0.1863	-0.026	0.2123	0.0032	0.36	3
	2115	42	14.110	0.2185	0.0352	0.1448	0.0285	0.29	
	2124	46	6.133	0.2056	-0.178	0.2388	0.0699	2.16	
	2133	40	26.230	0.1387	0.0438	0.1355	0.0254	1.07	
	2135	43	1.460	0.1748	0.1123	0.0927	0.0252	0.67	
	2140	18	259.06	0.2032	0.1472	0.1818	0.0729	0.81	
	2145	45	13.042	0.1672	0.0727	0.1220	0.0676	0.39	
	2151	43	11.006	0.1870	0.0560	0.0778	0.0345	0.62	
	2154	39	2.673	0.2362	0.1262	0.1070	0.0571	1	
	2155	19	2.945	0.1594	-0.089	0.2819	0.0187	1.77	
	2157	39	1.805	0.2420	0.0705	0.1375	0.0227	0.96	
	2158	38	2.333	0.1336	-0.035	0.1837	0.0614	1.17	
	2164	38	1.840	0.2200	-0.052	0.1133	0.0447	0.89	
	2167	22	2.589	0.1662	0.0206	0.1149	-0.0056	0.46	
	2174	20	21.331	0.2099	-0.013	0.0965	-0.0248	0.63	
	2177	22	5.383	0.1872	0.2167	0.2397	0.1837	2.77	
	Regional	**_**	**34.26**	**0.191**	**0.029**	**0.147**	**0.043**	**_**	
Second Subregion	2125	16	1.749	0.310	0.251	0.240	0.096	0.88	1.33
	2131	46	0.386	0.305	0.104	0.075	0.083	1.29	
	2166	38	9.421	0.282	0.132	0.029	0.010	1.23	
	2168	25	0.138	0.337	0.221	0.200	0.046	1.18	
	2171	16	0.033	0.330	0.247	0.258	0.315	0.42	
	Regional	**_**	**2.345**	**0.308**	**0.165**	**0.124**	**0.11**	**_**	
Third Subregion	2119	38	22.377	0.132	0.045	0.129	0.089	1.050	1.33
	2147	33	13.494	0.107	0.253	0.095	0.017	0.790	
	2149	41	18.228	0.131	0.211	0.013	-0.016	1.300	
	2156	39	66.131	0.091	0.089	0.177	0.070	1.280	
	2172	26	8.245	0.122	0.175	0.118	-0.046	0.580	
	Regional	**_**	**25.7**	**0.116**	**0.151**	**0.098**	**0.023**	**_**	

According to Hosking and Wallis (1997), the region is declared heterogeneous if the value of H is sufficiently high, "acceptably homogeneous" if H<1, "possibly heterogeneous" if H <2, and "heterogeneous" if H > 2. The result of the sub-region of the Firat basin using both plotting position and unbiased estimators shows that all the sub-regions are acceptably homogeneous or possibly homogeneous, as shown in Table 4.4.

Table 4.4 Results of heterogeneous test for Firat basin.

Estimators	Region	No of stations	H_1	H_2	H_3
Plotting Position	**First Subregion**	16	0.9	-0.38	-1.51
	Second Subregion	5	-1.22	-0.18	0.45
	Third Subregion	5	0.58	0.15	0.2
Unbiased	**First Subregion**	16	1.36	0.71	-0.24
	Second Subregion	5	1.01	-0.31	1.28
	Third Subregion	5	1.97	1.7	1.23

For the distributions of generalized logistics, generalized extreme values, generalized normal, Pearson type III, and generalized pareto, the goodness-of-fit value, Z_{dist}, is computed. When the Z_{dist} is smaller than 1.64, the distribution can be considered a fit distribution, as shown in Table 4.5. As a result, the best-suited distribution is the closest |z| value to zero. In general, all distributions with |z|<1.64 are appropriate.

Table 4.5 Z Test's Results for Firat basin

Estimators	**Distributions**	**Z_{DIST}**					
		Region-1		**Region -2**		**Region -3**	
		L-kurt	Z_{dist}	L-kurt	Z_{dist}	L-kurt	Z_{dist}
Plotting Position	**GLO**	0.169	0.1	0.189	1.83	0.186	1.07
	GEV	0.115	-3.09	0.147	0.56	0.144	-0.34
	GNO	0.125	-2.49	0.143	0.44	0.141	-0.43
	PE3	0.123	-2.58	0.131	0.06	0.13	-0.79
	GPA	0.012	-9.13	0.057	-2.19	0.053	-3.34
Unbiased	**GLO**	0.167	1.21	0.189	2.05	0.186	3.47
	GEV	0.111	-2.33	0.148	0.77	0.143	1.78
	GNO	0.123	-1.54	0.144	0.65	0.141	1.69
	PE3	0.123	-1.6	0.131	0.25	0.13	1.26
	GPA	0.007	-8.88	0.059	-2.01	0.052	-1.83

Table 4.6 and Table 4.7 present the quantile function for the Firat Basin based on Plotting Position estimators and unbiased estimators. This table provides a comprehensive representation of data distribution in the Firat Basin, calculated using different plotting position methods. A quantile function is a statistical tool that describes the values that divide a set of observations into different intervals. In this case, the quantile function gives a clear picture of how the data in the Firat Basin is distributed, and how the difference between Plotting Position estimators and unbiased estimators can be used to estimate the quantiles of the distribution. The table is useful for understanding the patterns and trends in the data and can be used as a reference for further analysis and decision-making.

Table 4.6 Quantile Function for Firat Basin depending on Plotting Position estimators.

Sub Region	F	0.100	0.200	0.500	0.800	0.900	0.960	0.980	0.990	0.995	0.998	0.999
	Y	-0.83	-0.47	0.367	1.500	2.250	3.199	3.902	4.600	5.296	6.214	6.907
	T	1.111	1.25	2	5	10	25	50	100	200	500	1000
First Subregion	GLO	0.582	0.726	0.984	1.261	1.432	1.648	1.812	1.98	2.152	2.387	2.572
	WAKEBY	0.547	0.727	0.985	1.26	1.446	1.667	1.819	1.958	2.085	2.237	2.341
	Observed Values	0.641	0.730	0.941	1.224	1.412	1.649	1.825	2.000	2.174	2.404	2.577
Second Subregion	GEV	0.371	0.532	0.91	1.413	1.742	2.154	2.457	2.756	3.051	3.436	3.725
	GNO	0.368	0.529	0.91	1.416	1.743	2.149	2.447	2.743	3.038	3.43	3.73
	PE III	0.365	0.521	0.909	1.426	1.753	2.146	2.426	2.694	2.955	3.289	3.537

Table 4.6 (Continue)

Second Subregion	WAKEBY	0.34	0.496	0.93	1.409	1.699	2.1	2.436	2.808	3.222	3.841	4.371
	Observed Values	0.408	0.555	0.902	1.368	1.676	2.066	2.355	2.642	2.928	3.305	3.590
Third Subregion	GLO	0.751	0.823	0.97	1.15	1.276	1.449	1.593	1.751	1.925	2.185	2.408
	GEV	0.749	0.815	0.966	1.165	1.294	1.453	1.568	1.68	1.79	1.932	2.037
	GNO	0.748	0.814	0.967	1.166	1.293	1.45	1.565	1.677	1.789	1.937	2.05
	PE III	0.747	0.811	0.966	1.17	1.297	1.449	1.557	1.66	1.76	1.888	1.983
	WAKEBY	0.758	0.828	0.959	1.169	1.306	1.463	1.565	1.654	1.733	1.823	1.882
	Observed Values	0.754	0.823	0.975	1.159	1.268	1.390	1.471	1.541	1.603	1.670	1.711

Table 4.7 Quantile Function for Firat Basin depending on Unbiased estimators.

Sub Region	F	0.100	0.200	0.500	0.800	0.900	0.960	0.980	0.990	0.995	0.998	0.999
	Y	-0.83	-0.47	0.367	1.500	2.250	3.199	3.902	4.600	5.296	6.214	6.907
	T	1.111	1.25	2	5	10	25	50	100	200	500	1000
First Subregion	GLO	0.586	0.732	0.991	1.26	1.423	1.624	1.775	1.926	2.079	2.285	2.445
	GNO	0.574	0.713	0.99	1.281	1.439	1.612	1.726	1.831	1.928	2.048	2.133
	PE III	0.574	0.713	0.99	1.281	1.439	1.612	1.726	1.83	1.927	2.046	2.13
	WAKEBY	0.538	0.711	1.003	1.256	1.423	1.63	1.778	1.919	2.053	2.219	2.338
	Observed Values	0.641	0.730	0.941	1.224	1.412	1.649	1.825	2.000	2.174	2.404	2.577
Second Subregion	GEV	0.371	0.532	0.909	1.412	1.743	2.159	2.465	2.768	3.068	3.461	3.757
	GNO	0.369	0.528	0.909	1.416	1.744	2.154	2.455	2.754	3.052	3.45	3.755
	PE III	0.365	0.52	0.907	1.426	1.755	2.151	2.432	2.703	2.966	3.304	3.554
	WAKEBY	0.342	0.492	0.927	1.417	1.702	2.089	2.419	2.793	3.219	3.878	4.46
	Observed Values	0.408	0.555	0.902	1.368	1.676	2.066	2.355	2.642	2.928	3.305	3.590
Third Subregion	PE III	0.757	0.819	0.968	1.163	1.284	1.429	1.532	1.63	1.725	1.847	1.937
	WAKEBY	0.756	0.816	0.963	1.176	1.301	1.429	1.503	1.563	1.611	1.661	1.69
	Observed Values	0.754	0.823	0.975	1.159	1.268	1.390	1.471	1.541	1.603	1.670	1.711

Table 4.8 and Table 4.9 show the accuracy measures of the Regional Growth Curve for the Firat Region based on plotting position and unbiased estimators. This table provides a comprehensive evaluation of the performance of different estimators in estimating the growth of the Firat Region. The accuracy measures listed in the table, such as errors of rates bounds and Root Mean Square Error (RMSE), provide insights into how well the estimators fit the observed data. A lower value of these accuracy measures indicates a better fit, and thus a more accurate representation of the growth of the Firat Region. These tables are useful for understanding the strengths and weaknesses of different estimators and for selecting the best estimator for a particular analysis or decision-making process. The results in this table can also be used as a reference for comparison with other regions or for future studies.

Table 4.8. Accuracy Measures of the Regional Growth Curve for the Firat Region depending on Plotting Position estimators.

Sub Region	Fit distribution	F	0.1	0.2	0.5	0.8	0.9	0.96	0.99	0.995	0.998	0.999
		Y	-0.83	-0.47	0.367	1.500	2.250	3.199	3.902	4.600	5.296	6.214
		T	1.111	1.25	2	5	10	25	100	200	500	1000
First Subregion	GLO	q(F)	0.582	0.726	0.984	1.261	1.432	1.648	1.979	2.151	2.387	2.572
		RMSE	0.083	0.045	0.015	0.025	0.036	0.051	0.076	0.09	0.11	0.126
		95%	0.53	0.688	0.962	1.219	1.365	1.526	1.756	1.863	2	2.096
		5%	0.656	0.773	1.009	1.298	1.496	1.757	2.187	2.419	2.755	3.029
		Different	0.126	0.085	0.047	0.079	0.131	0.231	0.431	0.556	0.755	0.933
Second Subregion	PE III	q(F)	0.365	0.521	0.909	1.426	1.753	2.146	2.694	2.955	3.289	3.537
		RMSE	0.151	0.093	0.044	0.026	0.048	0.075	0.108	0.122	0.138	0.149
		95%	0.289	0.451	0.856	1.374	1.632	1.902	2.236	2.383	2.59	2.742
		5%	0.465	0.603	0.99	1.494	1.898	2.427	3.198	3.577	4.086	4.467
		Different	0.176	0.152	0.134	0.12	0.266	0.525	0.962	1.194	1.496	1.725
Third Subregion	GEV	q(F)	0.749	0.815	0.966	1.165	1.294	1.452	1.68	1.79	1.932	2.037
		RMSE	0.036	0.025	0.015	0.016	0.026	0.047	0.089	0.114	0.15	0.181
		95%	0.71	0.785	0.943	1.14	1.245	1.347	1.44	1.475	1.486	1.49
		5%	0.788	0.847	0.992	1.194	1.348	1.565	1.902	2.084	2.337	2.546
		Different	0.078	0.062	0.049	0.054	0.103	0.218	0.462	0.609	0.851	1.056

Table 4.9 Accuracy Measures of the Regional Growth Curve for the Firat Region depending on Unbiased estimators.

Sub Region	Fit distribution	F	0.1	0.2	0.5	0.8	0.9	0.96	0.99	0.995	0.998	0.999
		Y	-0.83	-0.47	0.367	1.500	2.250	3.199	3.902	4.600	5.296	6.214
		T	1.111	1.25	2	5	10	25	100	200	500	1000
First Subregion	GLO	q(F)	0.586	0.732	0.991	1.26	1.422	1.624	1.925	2.079	2.285	2.444
		RMSE	0.087	0.045	0.014	0.026	0.036	0.05	0.072	0.084	0.101	0.115
		95%	0.533	0.698	0.97	1.212	1.35	1.509	1.719	1.807	1.926	2.02
		5%	0.671	0.783	1.015	1.298	1.481	1.717	2.104	2.305	2.591	2.823
		Different	0.138	0.085	0.045	0.086	0.131	0.208	0.385	0.498	0.665	0.803
Second Subregion	PE III	q(F)	0.365	0.151	0.289	0.465	0.176	0.365	0.151	0.289	0.465	0.176
		RMSE	0.52	0.093	0.451	0.6	0.149	0.52	0.093	0.451	0.6	0.149
		95%	0.907	0.044	0.854	0.99	0.136	0.907	0.044	0.854	0.99	0.136
		5%	1.427	0.026	1.374	1.494	0.12	1.427	0.026	1.374	1.494	0.12
		Different	1.755	0.048	1.635	1.901	0.266	1.755	0.048	1.635	1.901	0.266
Third Subregion	PE III	q(F)	0.757	0.819	0.968	1.163	1.284	1.429	1.63	1.725	1.847	1.937
		RMSE	0.033	0.025	0.015	0.014	0.027	0.045	0.069	0.08	0.093	0.102
		95%	0.721	0.789	0.946	1.14	1.232	1.331	1.456	1.511	1.577	1.631
		5%	0.793	0.851	0.994	1.189	1.337	1.531	1.806	1.942	2.117	2.256
		Different	0.072	0.062	0.048	0.049	0.105	0.2	0.35	0.431	0.54	0.625

Standardized quantiles have been computed for the selected return periods of T = 1.11, 1.25, 2, 5, 10, 20, 100, 200, 500, and 1000 years, using the proper distribution for all sub-regions, then

plotted against the relevant return periods. (Figure 4.4) shows the growth curves depending on the plotting position and unbiased estimator.

This figure provides a graphical representation of the data distribution in the Firat Basin, calculated using different estimators. A frequency curve is a tool that shows the relative frequency or probability of occurrences of different values in a set of observations. In this case, the frequency curves show how the data in the Firat Basin is distributed and how different estimators can be used to estimate the distribution. The figure helps in understanding the patterns and trends in the data. The comparison of different frequency curves can also reveal the similarities and differences in the distribution of data, which can help select the best estimator for a particular analysis.

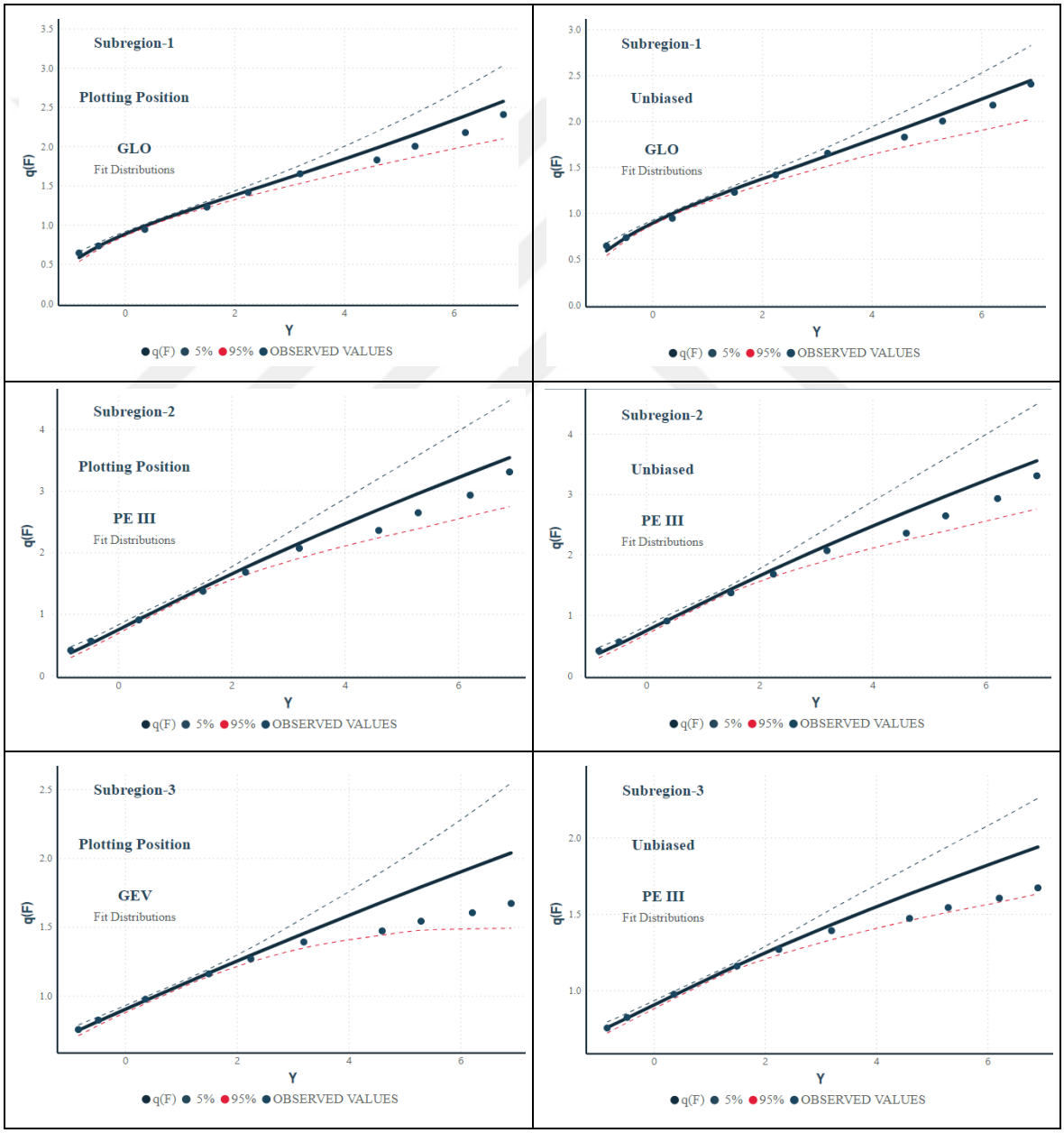

Figure 4.4. Frequency Curves of the Firat Basin depend on Plotting Position and Unbiased estimators.

4.2 The Dicle basin stations

The Dicle River Basin in Turkey is subjected to a regional frequency of low flow study utilizing the index flood procedure coupled with the L-moments approach employing the yearly low flow peak series of 16 stream-gauging stations in the Dicle basin. Records of the Dicle River's annual minimum streamflow from 16 sites are included in the data collection. The General Directorate of Electrical Power Resources Survey and Development Administration (EIE), which has records on minimal streamflow from 1961 to 2007, made this information public. The study period ranged from 16 to 45 years, with an average of 27 years of record per site, depending on the station location and data accessibility. The station names and details are displayed in Table 4.10. The geographical distribution of the stations in the basin is depicted in Figure 4.5.

Table 4.10 Used Stations in Dicle Basin

No	Station Name	Area km^2	Elevation	Q_{mean}	(E)	(N)
2603	Garzan Stream	2450	545	2.2	41.3	38.0
2605	Diyarbakir	5655	570	7.5	40.2	37.9
2606	Cizre	38281	370	99.7	42.2	37.4
2610	Baykan	640	910	2.7	41.8	38.2
2612	Batman Stream	4105	597	3.2	41.2	38.2
2617	Cayonu	1186	725	1.3	40.0	38.3
2618	Ambar Stream	976	595	0.2	40.4	38.0
2619	Goksu Stream	667	610	0.3	40.4	37.7
2620	Zap Water - Uzumcu	5344	1072	11.3	43.6	37.5
2621	zap Water - Musahan	2504	1725	3.4	44.1	37.8
2624	Kezer Stream	1170	700	2.4	41.9	38.0
2625	Hezil Stream	1127	880	2.3	42.7	37.5
2626	Botani Stream	7989	460	37.4	41.9	37.8
2627	Zap Water - Narli	677	775	21.9	43.6	37.3
2630	Zap Water -Teknisyenler	4172	1412	7.1	44.6	37.3
2631	Catak Water	2455	1482	6.8	43.2	37.7

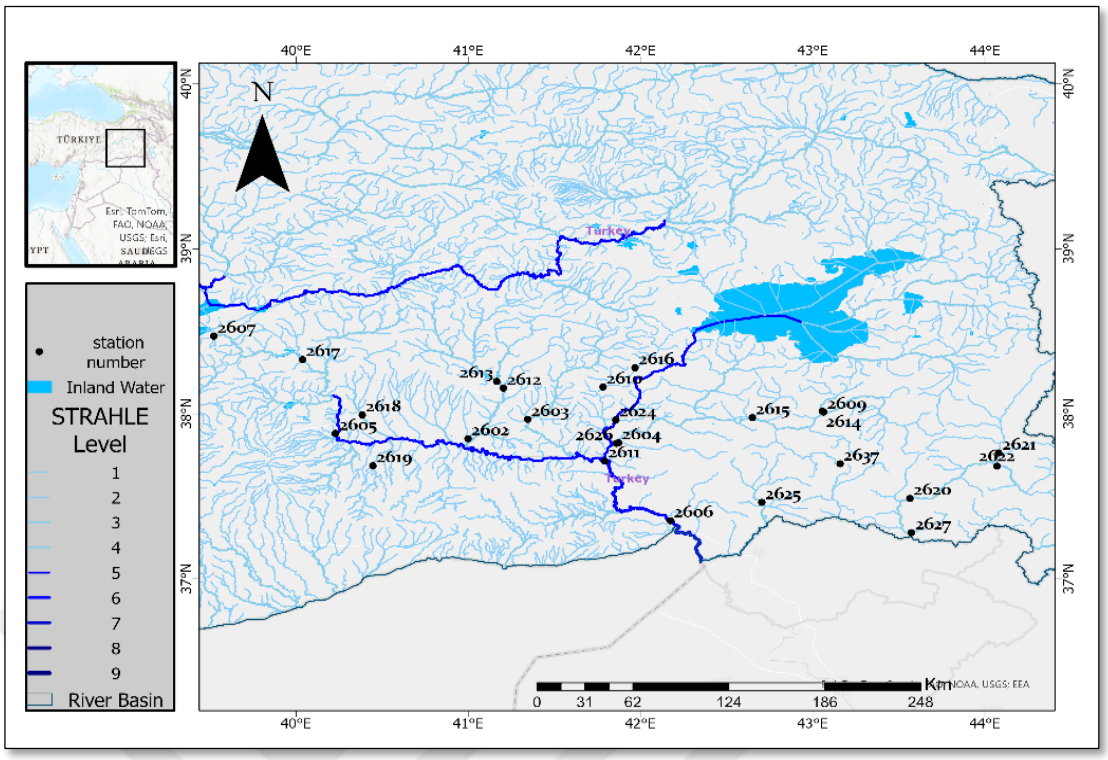

Figure 4.5 Geographical distribution of stations in the Dicle basin

A regional frequency of low flow analysis utilizing the index flood procedure paired with the L-moments approach is applied to the Firat rivers basin in Turkey using the yearly low flow peak series of 16 stream-gauging stations. L-moments Values were calculated using plotting position estimators and unbiased estimators using Excel. Figure 4.6 depicts the relationship between τ_1 and τ_3 for all stations.

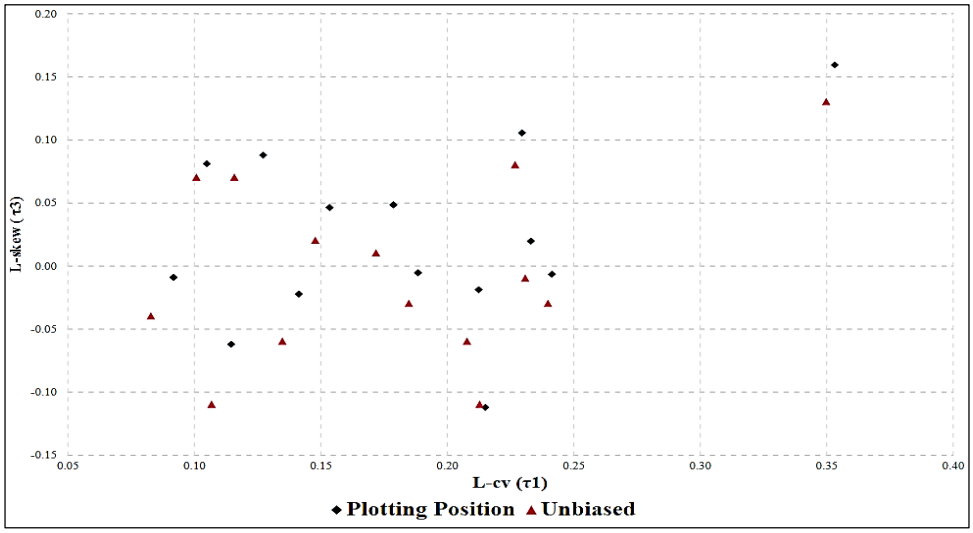

Figure 4.6 The relationship between τ_1 and τ_3 for all stations in Dicle Basin

The heterogeneity measures, H (1), H (2), and H (3), were estimated using 500 simulations utilizing data from 16 sites. based on unbiased estimators H values are (14.14), (3.32), and (1.04).

while depending on Plotting Position Estimators H Values are (13.62), (2.38), and (0.24). Because H (1), H (2), and H (3) are all greater than 2.0, these numbers imply that the Dicle River Basin is a heterogenous zone (Hosking and Wallis 1997). To define the homogeneous region, the area was divided into two sub-regions. During this process, two stations were excluded to ensure the formation of homogeneous regions, resulting in the inclusion of only 14 stations in the final analysis. Figure 4.7 depicts the distribution of stations based on τ_1 and τ_3 values.

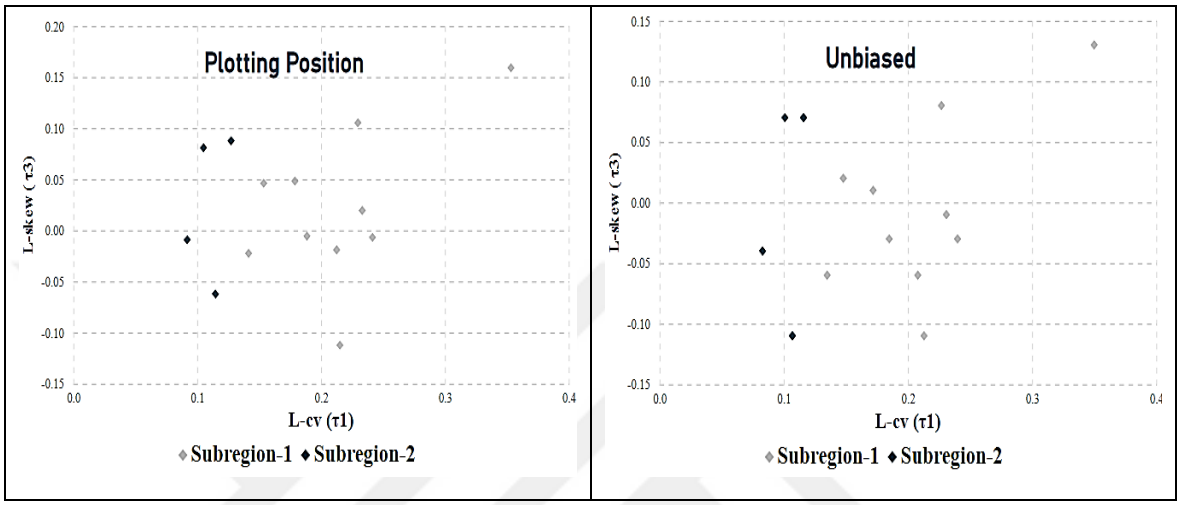

Figure 4.7 The relationship between τ_1 and τ_3 for *subregions* in Dicle Basin.

Table 4.11 shows the values of τ_1(L-cv), τ_3 (L-skew), and the discordancy measure Di for 16 stations. All calculations were computed for the subregion using Hosking's Fortran computer software (1991). The L-cv and L-skew values estimated from the recorded sample series of these 16 stations are based on the plotting position estimators. The results show that all Di values are less than the crucial value.

Table 4.11 L-Moments Values for the Dicle Basin depend on plotting position estimators.

Sub Region	Station	Record length	Mean	τ_1	τ_3	τ_4	τ_5	D_i	D_c
First Subregion	2603	37	2.32	0.242	-0.007	0.187	0.042	0.51	2.49
	2605	28	7.52	0.233	0.019	0.066	0.041	1.1	
	2617	28	1.31	0.230	0.105	0.154	0.073	0.53	
	2619	18	0.25	0.353	0.159	0.062	-0.007	2.22	
	2621	28	3.443	0.215	-0.112	0.153	-0.001	1.68	
	2624	34	2.416	0.154	0.046	0.253	0.074	1.14	
	2625	26	2.281	0.189	-0.006	0.253	0.129	0.79	
	2627	16	21.94	0.142	-0.022	0.173	0.013	0.83	
	2630	21	7.086	0.213	-0.019	0.204	0.020	0.34	
	2631	19	6.831	0.179	0.048	0.129	0.040	0.86	
	Regional	_	**4.727**	**0.212**	**0.013**	**0.17**	**0.042**	_	

Table 4.11(Continue)

Second Subregion	2606	25	99.71	0.092	-0.009	0.224	0.016	1	1
	2610	45	2.661	0.105	0.081	0.124	0.103	1	
	2626	26	37.37	0.115	-0.062	0.197	-0.090	1	
	2627	16	21.94	0.127	0.088	0.243	0.051	1	
	Regional	**_**	**40.22**	**0.108**	**0.029**	**0.18**	**0.02**	**_**	

Table 4.12 shows the values of τ_1(L-cv), τ_3 (L-skew), and the discordancy measure Di for 16 stations. All calculations were computed for the subregion using Hosking's Fortran computer software (1991). The L-cv and L-skew values estimated from the recorded sample series of these 16 stations are based on unbiased estimators. The results show that all Di values are less than the crucial value.

Table 4.12 L-Moment Values for Dicle basin depending on unbiased estimators.

Sub Region	**Station**	**Record length**	**Mean**	τ_1	τ_3	τ_4	τ_5	D_i	D_c
First Subregion	2603	37	2.32	0.24	-0.03	0.186	0.346	0.47	2.49
	2605	28	7.52	0.231	-0.01	0.031	0.017	0.83	
	2617	28	1.31	0.227	0.08	0.135	-0.06	0.63	
	2619	18	0.25	0.35	0.13	0.02	-0.02	2.2	
	2621	28	3.443	0.213	-0.11	0.146	-0.61	1.63	
	2624	34	2.416	0.148	0.02	0.241	0.095	1.16	
	2625	26	2.281	0.185	-0.03	0.257	0.151	0.78	
	2627	16	21.94	0.135	-0.06	0.131	0.048	0.89	
	2630	21	7.086	0.208	-0.06	0.204	0.035	0.42	
	2631	19	6.831	0.172	0.01	0.07	0.008	1	
	Regional	**_**	**4.727**	**0.209**	**-0.017**	**0.151**	**0.001**	**_**	
Second Subregion	2606	25	99.71	0.083	-0.04	0.142	0.032	1	1
	2610	45	2.661	0.101	0.07	0.192	0.117	1	
	2626	26	37.37	0.107	-0.11	0.143	-0.01	1	
	2627	16	21.94	0.116	0.07	0.168	0.047	1	
	Regional	**_**	**40.22**	**0.101**	**0.038**	**0.166**	**0.047**	**_**	

According to Hosking and Wallis (1997), the region is declared heterogeneous if the value of H is sufficiently high, "acceptably homogeneous" if H<1, "possibly heterogeneous" if H <2, and "heterogeneous" if H > 2. The result of the sub-region of the Dicle basin using both plotting position and unbiased estimators shows that all the sub-regions are acceptably homogeneous or possibly homogeneous, as shown in Table 4.13.

Table 4.13 Result of heterogeneous test for Dicle basin.

Estimators	**Region**	**No of stations**	H_1	H_2	H_3
Plotting Position	**First Subregion**	10	1.65	-1.09	-1.32
	Second Subregion	4	-0.42	-0.37	-0.51
Unbiased	**First Subregion**	10	1.89	-0.6	-0.28
	Second Subregion	4	-0.4	0.08	-0.54

For the distributions of generalized logistics, generalized extreme values, generalized normal, Pearson type III, and generalized pareto, the goodness-of-fit value, Z_{dist}, is computed. When the Z_{dist} is smaller than 1.64, the distribution can be considered a fit distribution, as shown in Table 4.14. As a result, the best-suited distribution is the closest |z| value to zero. In general, all distributions with $| Z_{dist} | < 1.64$ are appropriate.

Table 4.14 Z Test's Results for Dicle basin

Estimators	**Distributions**	**$\|Z_{dist}\|$**			
		Region-1		**Region -2**	
		L-kurt	Z_{dist}	L-kurt	Z_{dist}
Plotting Position	**GLO**	0.167	-0.37	0.167	-0.74
	GEV	0.109	-2.88	0.111	-2.23
	GNO	0.123	-2.26	0.123	-1.9
	PE3	0.122	-2.28	0.123	-1.92
	GPA	0.003	-7.43	0.007	-4.98
Unbiased	**GLO**	0.167	0.61	0.167	-0.04
	GEV	0.105	-2.16	0.107	-1.62
	GNO	0.123	-1.37	0.123	-1.21
	PE3	0.122	-1.39	0.122	-1.22
	GPA	-0.003	-7.05	0.001	-4.47

Table 4.15 and Table 4.16 present the quantile function for the Dicle Basin based on Plotting Position estimators and unbiased estimators. This table provides a comprehensive representation of data distribution in the Dicle Basin, calculated using different plotting position methods. A quantile function is a statistical tool that describes the values that divide a set of observations into different intervals. In this case, the quantile function gives a clear picture of how the data in the Dicle Basin is distributed, and how the difference between Plotting Position estimators and unbiased estimators can be used to estimate the quantiles of the distribution. The table is useful for understanding the patterns and trends in the data and can be used as a reference for further analysis and decision-making.

Table 4.15 Quantile Function for Dicle Basin depending on Plotting Position estimators

Sub Region	F	0.100	0.200	0.500	0.800	0.900	0.960	0.980	0.990	0.995	0.998	0.999
	Y	-0.83	-0.47	0.367	1.500	2.250	3.199	3.902	4.600	5.296	6.214	6.907
	T	1.111	1.25	2	5	10	25	50	100	200	500	1000
First Subregion	GLO	0.536	0.704	0.996	1.292	1.468	1.683	1.841	1.998	2.156	2.365	2.525
	WAKEBY	0.477	0.691	1.011	1.273	1.456	1.696	1.876	2.055	2.232	2.466	2.641
	Observed Values	0.516	0.684	1.002	1.296	1.436	1.589	1.706	1.843	2.017	2.331	2.652
Second Subregion	GLO	0.766	0.849	0.995	1.147	1.239	1.352	1.437	1.523	1.609	1.725	1.816
	WAKEBY	0.743	0.852	0.997	1.14	1.24	1.364	1.454	1.538	1.619	1.72	1.792
	Observed Values	0.767	0.850	1.001	1.135	1.201	1.283	1.358	1.456	1.590	1.837	2.093

Table 4.16 Quantile Function for Dicle Basin depending on Unbiased estimators.

Sub Region	F	0.100	0.200	0.500	0.800	0.900	0.960	0.980	0.990	0.995	0.998	0.999
	Y	-0.83	-0.47	0.367	1.500	2.250	3.199	3.902	4.600	5.296	6.214	6.907
	T	1.111	1.25	2	5	10	25	50	100	200	500	1000
First Subregion	GLO	0.539	0.713	1.006	1.292	1.455	1.65	1.79	1.926	2.06	2.233	2.362
	GNO	0.522	0.691	1.007	1.313	1.469	1.634	1.738	1.831	1.916	2.017	2.087
	PE III	0.522	0.691	1.007	1.313	1.47	1.634	1.738	1.831	1.915	2.016	2.086
	WAKEBY	0.492	0.712	1.005	1.297	1.474	1.662	1.777	1.872	1.951	2.036	2.087
	Observed Values	0.516	0.684	1.002	1.296	1.436	1.589	1.706	1.843	2.017	2.331	2.652
Second Subregion	GLO	0.779	0.86	0.999	1.139	1.221	1.321	1.393	1.465	1.537	1.631	1.703
	GEV	0.771	0.847	0.999	1.154	1.233	1.312	1.359	1.397	1.428	1.461	1.481
	GNO	0.772	0.85	0.999	1.15	1.229	1.313	1.368	1.418	1.463	1.518	1.557
	PE III	0.772	0.85	0.999	1.15	1.229	1.313	1.368	1.418	1.463	1.518	1.557
	WAKEBY	0.748	0.849	1.011	1.127	1.209	1.321	1.411	1.506	1.604	1.742	1.851
	Observed Values	0.767	0.850	1.001	1.135	1.201	1.283	1.358	1.456	1.590	1.837	2.093

Table 4.17 and Table 4.18 show the accuracy measures of the Regional Growth Curve for the Dicle Region based on plotting position and unbiased estimators. This table provides a comprehensive evaluation of the performance of different estimators in estimating the growth of the Dicle Region. The accuracy measures listed in the table, such as errors of rates bounds and Root Mean Square Error (RMSE), provide insights into how well the estimators fit the observed data. A lower value of these accuracy measures indicates a better fit, and thus a more accurate representation of the growth of the Dicle Region. These tables are useful for understanding the strengths and weaknesses of different estimators and for selecting the best estimator for a particular analysis or decision-making process. The results in this table can also be used as a reference for comparison with other regions or for future studies.

Table 4.17 Accuracy Measures of the Regional Growth Curve for the Dicle Region depending on Plotting Position estimators.

Sub Region	Fit distribution	F	0.1	0.2	0.5	0.8	0.9	0.96	0.99	0.995	0.998	0.999
		Y	-0.83	-0.47	0.367	1.500	2.250	3.199	3.902	4.600	5.296	6.214
		T	1.111	1.25	2	5	10	25	100	200	500	1000
First Subregion	GLO	q(F)	0.536	0.704	0.996	1.292	1.468	1.683	1.998	2.155	2.365	2.525
		RMSE	0.187	0.087	0.03	0.049	0.066	0.089	0.131	0.156	0.193	0.224
		95%	0.443	0.64	0.946	1.212	1.348	1.497	1.633	1.691	1.749	1.784
		5%	0.699	0.791	1.048	1.361	1.576	1.861	2.313	2.555	2.893	3.181
		Different	0.256	0.151	0.102	0.149	0.228	0.364	0.68	0.864	1.144	1.397
Second Subregion	GLO	q(F)	0.766	0.849	0.995	1.147	1.239	1.352	1.523	1.609	1.726	1.816
		RMSE	0.039	0.024	0.014	0.017	0.025	0.041	0.075	0.096	0.129	0.159
		95%	0.721	0.817	0.972	1.118	1.193	1.271	1.344	1.372	1.397	1.408
		5%	0.812	0.88	1.019	1.18	1.291	1.439	1.693	1.833	2.03	2.192
		Different	0.091	0.063	0.047	0.062	0.098	0.168	0.349	0.461	0.633	0.784

Table 4.18 Accuracy Measures of the Regional Growth Curve for the Dicle Region depending on Unbiased estimators.

Sub Region	Fit distribution	F	0.1	0.2	0.5	0.8	0.9	0.96	0.99	0.995	0.998	0.999
		Y	-0.83	-0.47	0.367	1.500	2.250	3.199	3.902	4.600	5.296	6.214
		T	1.111	1.25	2	5	10	25	100	200	500	1000
First Subregion	GLO	q(F)	0.539	0.713	1.006	1.292	1.455	1.65	1.926	2.06	2.233	2.362
		RMSE	0.198	0.087	0.03	0.051	0.067	0.088	0.124	0.146	0.177	0.204
		95%	0.441	0.649	0.954	1.206	1.332	1.469	1.589	1.648	1.688	1.705
		5%	0.727	0.803	1.056	1.363	1.566	1.82	2.206	2.404	2.682	2.904
		Different	0.286	0.154	0.102	0.157	0.234	0.351	0.617	0.756	0.994	1.199
Second Subregion	GLO	q(F)	0.779	0.86	0.999	1.139	1.221	1.321	1.465	1.537	1.631	1.703
		RMSE	0.041	0.023	0.014	0.018	0.025	0.039	0.069	0.087	0.116	0.141
		95%	0.732	0.829	0.976	1.11	1.176	1.242	1.302	1.33	1.348	1.357
		5%	0.828	0.892	1.023	1.173	1.272	1.404	1.617	1.73	1.886	2.015
		Different	0.096	0.063	0.047	0.063	0.096	0.162	0.315	0.4	0.538	0.658

Standardized quantiles have been computed for the selected return periods of T = 1.11, 1.25, 2, 5, 10, 20, 100, 200, 500, and 1000 years, using the proper distribution for all sub-regions, then plotted against the relevant return periods. (Figure 4.8) shows the results depending on the plotting position and unbiased estimator.

This figure provides a graphical representation of the data distribution in the Dicle Basin, calculated using different estimators. A frequency curve is a tool that shows the relative frequency or probability of occurrences of different values in a set of observations. In this case, the frequency curves show how the data in the Dicle Basin is distributed and how different estimators can be used to estimate the distribution.

The figure helps in understanding the patterns and trends in the data. The comparison of different frequency curves can also reveal the similarities and differences in the distribution of data, which can be helpful in selecting the best estimator for a particular analysis.

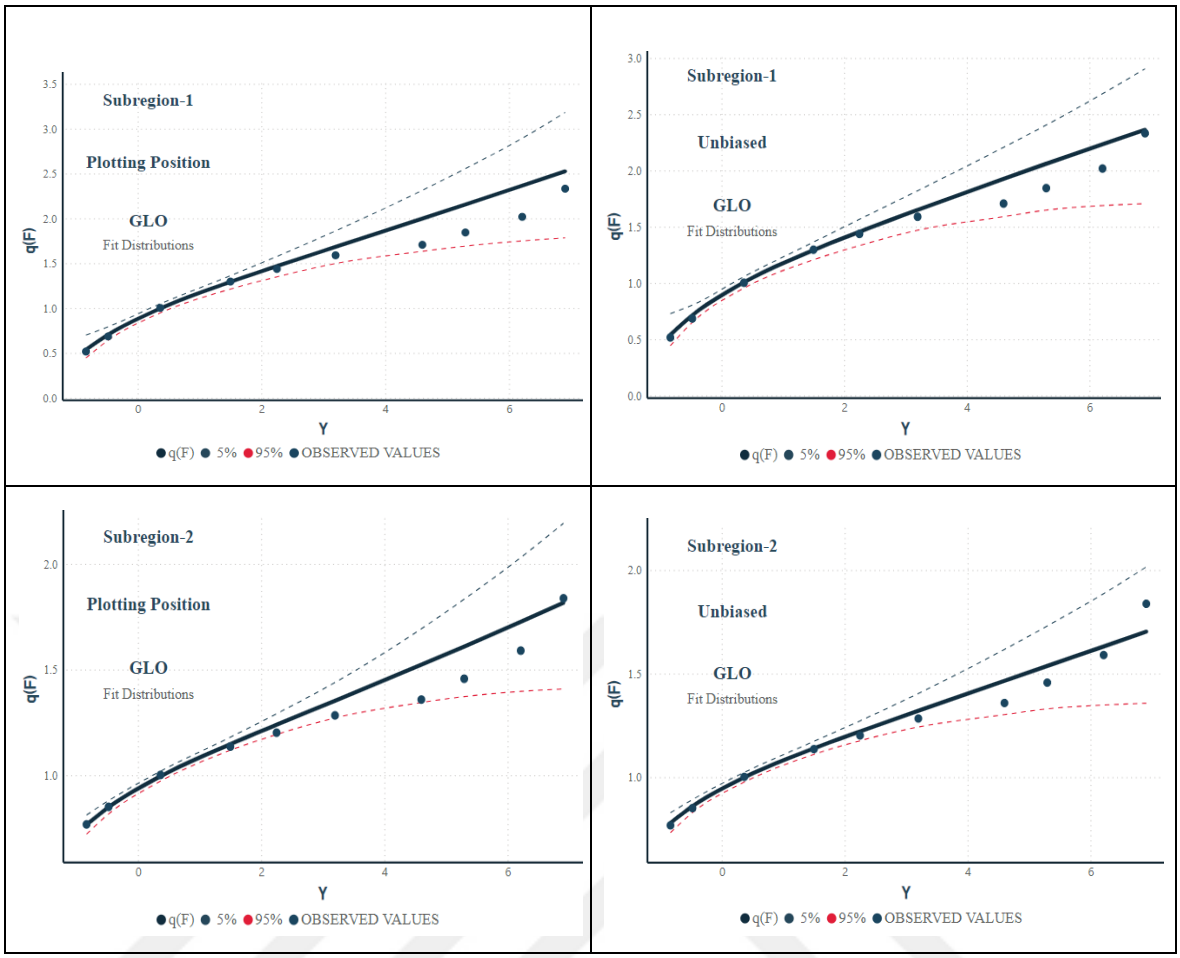

Figure 4.8 Frequency Curves of Dicle Basin depend on Unbiased estimators and Unbiased estimators.

5. CONCLUSION

This study aimed to determine regional frequency analysis for two catchment areas in Turkey; the first one was the Firat Basin, which contains about 20 rivers. The second one was the Dicle Basin, which has about 15 rivers. In both areas, two methods were applied for getting the L-moments to depend on the unbiased and plotting position methods. According to the study, the following results were got:

1- Depending on the result of the homogeneity test, the Firat basin is considered heterogeneous; therefore, the basin is divided into three sub-regions to define the homogeneous region depending on both unbiased and plotting position estimators.
2- Depending on the result of the homogeneity test, the Dicle basin is considered heterogeneous; therefore, the basin is divided into two sub-regions to define the homogeneous region depending on both unbiased and plotting position estimators.
3- For the Firat basin, the fit distribution in the first subregion is GLO, in the second subregion it is PE III, and in the third subregion it is GEV based on Plotting Position estimator. Based on Unbiased estimator, the fit distribution in the first subregion is GLO, in the second subregion is PE III, and in the third subregion it is also PE III. For the Dicle basin (Gen. Logistic), distribution was most appropriate for the first and second sub-regions, the same result was concluded depending on plotting position estimators.
4- Unbiased estimators demonstrated a slight advantage over plotting position estimators for quantile estimates in the Dicle and Firat basins, as reflected by RMSE values. Specifically, the average RMSE for the Firat region using unbiased estimators was 0.69, compared to 0.77 for plotting position estimators. The average RMSE for the Dicle region using unbiased estimators was 0.87, compared to 0.92 for plotting position estimators. This advantage of the Unbiased estimator was more evident in the upper quantile. The following Table 5.1 shows the RMSE values in each of the subregions for the Upper Quantile and the Lower Quantile.

Table 5.1 RMSE values in each of the subregions for the Upper Quantile and the Lower Quantile.

Region	Estimator	Plotting Position Estimator		Unbiased Estimator	
	Sub Region	Upper Quantile q(F)>0.995	Lower Quantile q(F)<0.5	Upper Quantile q(F)>0.995	Lower Quantile q(F)<0.5
Firat Basin	First Subregion	0.107	0.048	0.1	0.049
	Second Subregion	0.136	0.096	0.136	0.096
	Third Subregion	0.148	0.025	0.092	0.024
Dicle Basin	First Subregion	0.191	0.101	0.175	0.105
	Second Subregion	0.128	0.026	0.114	0.026

5- Given that plotting position estimators are simpler to calculate than unbiased estimators, as they rely on the ordering and ranking of the data, further studies could be conducted on larger samples. By comparing the differences in RMSE values, it may be possible to identify a critical value or threshold beyond which the plotting position estimator becomes preferable over the unbiased estimator for large studied samples. This would help refine the selection of the most appropriate estimation method depending on sample size and distribution characteristics.

6- Frequency curves for each region and equations for these curves have been proposed according to the distribution that best fits the region. Even in regions with no measurement or short recorded stations, the charts can calculate the minimum flow rate after calculating the average flow due to the possibility of not exceeding any recurrence period.

REFERENCES

Adamowski K. Regional analysis of annual maximum and partial flood data by nonparametric and L-moments methods. J Hydrol 2000, 229, 219–231.

Ahmad, I., Yasin, M., Fawad, M., & Saghir, A. (2017). Regional frequency analysis of low flows using L. moments for Indus Basin, in Pakistan. Pakistan Journal of Science, 69(1), 75.

Asikoglu, O. L. (2018). Parent flood frequency distribution of Turkish Rivers. Polish Journal of Environmental Studies, 27(2), 529-539.

Atiem A. & Harmancioglu N.B. Assessment of regional floods using L-moments approach: the case of the River Nile. Water Resource Manage 2006, 20, 723–747.

Aydoğan, D., Kankal, M. U. R. A. T., & Önsoy, H. (2016). Regional flood frequency analysis for Çoruh Basin of Turkey with L-moments approach. Journal of Flood Risk Management, 9(1), 69-86.

Bayazit, M., B. Önoz, 2002. LL-moments for estimating low flow quantiles / Estimation des quantiles d'étiage grâce aux LL-moments. Hydrological Sciences Journal, 47; 707-720.

Bhunyan P.K., Panigrahy N., Kumar R. & Berndtsson R. Development of a regional non-dimensional return period flood model. Water Resource Manage 2010, 24, 1425–1439.

Borujeni S.C. & Sulaiman W.N.A. Development of L-moment based models for extreme flood events. Malays J Math Sci 2009, 3, (2), 281–296.

Caruso, B. S. (2000). Evaluation of low-flow frequency analysis methods. Journal of Hydrology (New Zealand), 19-47.

Charron, C., & Ouarda, T. B. (2015). Regional low-flow frequency analysis with a recession parameter from a nonlinear reservoir model. Journal of Hydrology, 524, 468-475.

Chen Y.D. Regional analysis of low flow using L-moments for Dongjiang Basin, South China. Hydrol Sci J 2006, 51, (6), 1051–1064.

Chowdhury J U & Stedinger J R (1991). Confidence interval for design flood with estimated skew coefficient. Journal of Hydraulic Engineering 117(7): 811–931

Dalrymple T. Flood frequency methods. U.S. Geological Survey Water Supply Paper, 1543A, 1960.

Dodangeh, E., S. Soltani, A. Sarhadi, J.T. Shiau, 2013. Application of L-moments and Bayesian inference for low-flow regionalization in Sefidroud basin, Iran. Hydrological Processes, 35; 1-14.

DSİ, 1994. Türkiye Akarsu Havzaları Maksimum Akımlar Frekans Analizi (MAFA). Ankara

DSI˙ (General Directorate of State Hydraulic Works). Official agenda. Ankara, Turkey, 2010.

Du, T., L. Xiong, Ch.Y. Xu, Ch.J. Gippel, S. Guo, P. Liu, 2015. Return period and risk analysis of nonstationary low-flow series under climate change. Journal of Hydrology, 527; 234–250.

Ellouze M, Abida H (2008) Regional flood frequency analysis in Tunisia: identification of regional distributions. Water Resour Manag 22(8):943–957

Eris, E., Aksoy, H., Onoz, B., Cetin, M., Yuce, M. I., Selek, B., ... & Karakus, E. U. (2019). Frequency analysis of low flows in intermittent and nonintermittent rivers from hydrological basins in Turkey. Water Supply, 19(1), 30-39.

Eslamian, S.S., S. Chavoshi, 2003. The Application of Lmoments Theory in Flood Frequency Analysis of Central Catchments of Iran. JWSS, 7; 1-17

Fisher, R. A., & Tippett, L. H. C. (1928). 063: Limiting Forms of the Frequency Distribution of the Largest of Smallest Member of a Sample.

Greenwood, J.A., J.M. Landwehr, N.C. Matalas, J.R.Wallis, 1979. Probability Weighted Moments: Definitions and Relation to Parameters of Several Distributions Expressible in Inverse Form. Water Resource Research, 15; 1049-1054.

Hall, M. J., & Minns, A. W. (1999). The classification of hydrologically homogeneous regions. Hydrological Sciences Journal, 44(5), 693-704.

Hosking J.R.M. & Wallis J.R. Regional frequency analysis: an approach based on L-moments. Cambridge, UK: Cambridge University Press, 1997.

Hosking J.R.M. & Wallis J.R. Some statistics useful in regional frequency analysis. Water Resource Res 1993, 29, (2), 271–281.

Hosking J.R.M. L-moments: analysis and estimation of distributions using linear combinations of order statistics. J R Stat Soc B 1990, 52, (1), 105–124.

Hosking J.R.M., Wallis R.J. & Wood E.F. Estimation of the generalized extreme value distribution by the method of probability weighted moments. Water Resources Research 1985, 31, (8), 2019–2025.

Hosking J.R.M., Wallis R.J. & Wood E.F. A Comparison of Unbiased and Plotting-Position Estimators of L Moments. Technometrics 1985, 27, (3), 251–261.

Hussain Z, Pasha GR (2009) Regional flood frequency analysis of the seven sites of Punjab, Pakistan, using L-moments. Water Resour Manag 23:1917–1933

Jingyi, Z., M.J. Hall, 2004. Regional Flood Frequency Analysis for the Gan-Ming River Basin in China. Journal of Hydrology, 296; 98-117.Keshtkar, A. (2015, p. 1).

Kil S L & Sang U K (2008). Identification of uncertainty in low flow frequency analysis using Bayesian MCMC method. Hydrological Processes 22(12): 1949-1964

Kim, S. U., & Lee, K. S. (2010). Regional low flow frequency analysis using Bayesian regression and prediction at ungauged catchment in Korea. KSCE Journal of Civil Engineering, 14(1), 87-98.

Kjeldsen, T.R., J.C. Smithers, R.E. Schulze, 2001. Regional Flood Frequency Analysis in the KwaZulu- Natal Province, South Africa, Using the Index-Flood Method. Journal of Hydrology, 255; 194-211.

Kroll, C.N., Vogel, R.M., 2002. Probability distribution of low streamflow series. Journal of Hydrological Engineering, ASCE, 7; 137–146.

Kumar, R., Chatterjee, C., Kumar, S., Lohani, A. K. and Singh, R. D. (2003). "Development of regional flood frequency relationships using L-moments for Middle Ganga Plains Subzone 1(f) of India." Water Resources Managament, 17, 4, 243–257.

Kumar, R., Chatterjee, C., Kumar, S., Lohani, A.K., Singh, R.D., 2003. Development of regional flood frequency relationships using L-moments for Middle Ganga Plains Subzone 1(f) of India. Water Resource Management, 17; 243–257.

Landwehr, J. M., Matalas, N. C., & Wallis, J. R. (1979). Probability weighted moments compared with some traditional techniques in estimating Gumbel parameters and quantiles. Water Resources Research, 15, 1055–1064.

Lin B., Bonnin G.M., Martin D.L., Parzybok T., Yekta M. & Riley D. Regional frequency studies of annual extreme precipitation in the United States based on regional L-moments analysis. In: Randall Graham, P.E., ed. Proceedings of EWRI2006. Omaha: ASCE, 2006, pp. 1–11.

Malekinezhad, H., H.P. Nachtnebel, A. Klik, 2011. Regionalization Approach for Extreme Flood Analysis Using L-moments. Journal of Agricultural Science and Technology, 13; 1183-1196.

Minocha, V.K., 2003. Discussion of Probability distribution of low streamflow series by C.N. Kroll & R.M. Vogel. Journal of Hydrologic Engineering, ASCE, 8; 297.

Modarres, R., 2008. Regional Frequency Distribution Type of Low Flow in North of Iran by L-moments. Water Resources Management, 22; 823-841.

Myung Suk Kim, 2008. On the Effects of Plotting Positions to the Probability Weighted Moments Method for the Generalized Logistic Distribution. The Korean Statistical Society, 14; 561-576.

Norbiato, D., Borga, M., Sangati, M., & Zanon, F. (2007). Regional frequency analysis of extreme precipitation in the eastern Italian Alps and the August 29, 2003 flash flood. Journal of hydrology, 345(3-4), 149-166.

Noto L.V. & Loggia G. L-moments approach for regional flood frequency analysis in Sicily, Italy. Water Resour Res 2009, 23, 2207–2229.

Ouarda TBMJ, Ba KM, Diaz-Delgado C, Carsteanu A, Chokmani K, Gingras H, Quentin E, Trujillo E, Bobee B (2008) Intercomparison of regional flood frequency estimation methods at ungauged sites for a Mexican case study. J Hydrol 348:40–58

Pearson C.P. New Zealand regional flood frequency analysis using L-moments. J Hydrol 1991, 30, (2), 53–64.

Peng, S., C. Xi, Q. Si-min, Y. Tao, Z. Zhi-cai, M. Jianliang, 2009. Regional Frequency Analysis of Low Flow Based on L-Moments in Karst Area, Southwest China. Joint International Convention of 8th IAHS Scientific Assembly and 37th IAH Congress, Water: A vital resource under stress – How science can help, September 6-12, Hyderabad, India.

Robert M. Hirsch, Jery R. Stedinger (1987). Plotting positions for historical floods and their precision. Water Resources Research, 23(4), 715-727.

Rustomji, P., Bennett, N., & Chiew, F. (2009). Flood variability east of Australia's Great Dividing Range. Journal of Hydrology, 374(3-4), 196-208.

Saf B. Regional flood frequency analysis using L moments for the Buyuk and Kucuk Menderes river basins of Turkey.

Saf B. Regional flood frequency analysis using L-moments for the West Mediterranean region of Turkey. Water Resour Res 2009a, 23, 531–551.

Sawaske, S.R., D.R. Freyberg, 2014. An analysis of trends in baseflow recession and low-flows in rain-dominated coastal streams of the pacific coast. Journal of Hydrology, 519; 599–610.

Schaefer, M.G. (1990). Regional analysis of precipitation annual maxima in Washington State, Water Resour. Res., 26(1), 191-131.

Seckin N., Cobaner M., Yurtal R. & Haktanir T. Comparison of artificial neural network methods with L-moments for estimating flood flow at ungauged sites: the case of East Mediterranean River basin, Turkey. Water Resource Manage 2013, 27, 2103–2124.

Seçkin, N., 2009, L-momentlere Dayali Gösterge-Sel Metodu ile Bölgesel Taşkin Frekans Analizi, University of Cukurova.

Seckin, N., Haktanir, T., & Yurtal, R. (2011). Flood frequency analysis of Turkey using L-moments method. Hydrological Process, 25, 3499–3505.

Shi P., Chen X., Qu S., Zhang Z. & Ma J. Regional frequency analysis low flow based on L moments: case study in Kars area, Southwest China. J Hydrol Eng 2010, 15, (5), 370–377.

Smakhtin, V.U., 2001. Low flow hydrology: a review. Journal of Hydrology, 240; 147–186.

Staudinger M, J. Seibert, 2014. Predictability of low flow – An assessment with simulation experiments. Journal of Hydrology, 519; 1383–1393.

Topaloğlu, F. (2005). Regional flood frequency analysis of the basins of the east mediterranean region. Turkish journal of agriculture and forestry, 29(4), 287-295.

Vogel R.M. & Fennessey N.M. L-moments should replace product moment diagrams. Water Resour Res 1993, 29, (6), 1745–1752.

Vogel R.M. & Wilson I. The probability distribution of annual maximum, mean and minimum streamflow's in the United States. J Hydrol Eng 1996, 1, (2), 69–76.

Vogel, R.M., N.M. Fennessey, 1993. L-moments diagrams should replace product-moment diagrams. Water Resource Research, 29; 1745-1752.

Vorapat Muangsuwan, Manad Khamkong, Putipong Bookkamana, 2017. Parameter Estimation of the Generalized Pareto Distribution By using a Plotting Position, 22, (3), 410–422.

Wallis J.R. & Wood E.F. Relative accuracy of log Pearson III procedures. J Hydraul Eng 1985, 111, (7), 1043–1056.

Zafirakou-Koulouris, A., Vogel, R. M., Craig, S. M., and Habermeier, J. (1998). "L-moment diagrams for censored observations." Water Resources Research, 34, 5, 1241-1249.

CURRICULUM VITAE

Mohammad Mosto. Attended Chemical Engineering Faculty of Al Baath University after graduating from Ibn Khaldoun School. But due to the war, he moved to Jordan, where he earned a Bachelor's degree in Civil Engineering in 2016. He later pursued and completed a Master's degree in Civil Engineering at Çukurova University in 2024. Mohammad has been working in the field of civil engineering within NGOs, gaining over five years of experience in management, data analysis, data science, and quality control.